




# Modulation of auxin signalling through *DIAGETROPICA* and *ENTIRE* differentially affects tomato plant growth via changes in photosynthetic and mitochondrial metabolism

Willian Batista-Silva<sup>1,2</sup>  | David B. Medeiros<sup>1,2</sup> | Acácio Rodrigues-Salvador<sup>1,2</sup> | Danilo M. Daloso<sup>3†</sup> | Rebeca P. Omena-Garcia<sup>1,2</sup> | Franciele Santos Oliveira<sup>1,2</sup> | Lilian Ellen Pino<sup>4</sup> | Lázaro Eustáquio Pereira Peres<sup>4</sup> | Adriano Nunes-Nesi<sup>1,2</sup>  | Alisdair R. Fernie<sup>3</sup> | Agustín Zsögön<sup>1</sup> | Wagner L. Araújo<sup>1,2</sup> 

<sup>1</sup>Departamento de Biologia Vegetal, Universidade Federal de Viçosa, Viçosa, Minas Gerais, Brazil

<sup>2</sup>Max-Planck Partner Group at the Departamento de Biologia Vegetal, Universidade Federal de Viçosa, Viçosa, Minas Gerais, Brazil

<sup>3</sup>Central Metabolism Group, Max Planck Institute of Molecular Plant Physiology, Potsdam-Golm, Germany

<sup>4</sup>Departamento de Ciências Biológicas, Escola Superior de Agricultura Luiz de Queiroz, Universidade de São Paulo, Piracicaba, Brazil

## Correspondence

Wagner L. Araújo, Departamento de Biologia Vegetal, Universidade Federal de Viçosa, Viçosa 36570-900, Minas Gerais, Brazil. Email: wlaraujo@ufv.br

## Present Address

<sup>†</sup>Departamento de Bioquímica e Biologia Molecular, Universidade Federal do Ceará, Fortaleza, Ceará, Brasil.

## Funding information

Fundação de Amparo à Pesquisa do Estado de Minas Gerais (FAPEMIG), Grant/Award Numbers: APQ-01357-14 and APQ-01078-15; Max-Planck-Gesellschaft; Brazilian Federal Agency for Support and Evaluation of Graduate Education (CAPES); Conselho Nacional de Desenvolvimento Científico e Tecnológico (CNPq); Foundation for Research Assistance of the São Paulo State (FAPESP), Grant/Award Number: 2014/16553-1

## Abstract

Auxin modulates a range of plant developmental processes including embryogenesis, organogenesis, and shoot and root development. Recent studies have shown that plant hormones also strongly influence metabolic networks, which results in altered growth phenotypes. Modulating auxin signalling pathways may therefore provide an opportunity to alter crop performance. Here, we performed a detailed physiological and metabolic characterization of tomato (*Solanum lycopersicum*) mutants with either increased (*entire*) or reduced (*diageotropica*—*dgt*) auxin signalling to investigate the consequences of altered auxin signalling on photosynthesis, water use, and primary metabolism. We show that reduced auxin sensitivity in *dgt* led to anatomical and physiological modifications, including altered stomatal distribution along the leaf blade and reduced stomatal conductance, resulting in clear reductions in both photosynthesis and water loss in detached leaves. By contrast, plants with higher auxin sensitivity (*entire*) increased the photosynthetic capacity, as deduced by higher  $V_{cmax}$  and  $J_{max}$  coupled with reduced stomatal limitation. Remarkably, our results demonstrate that auxin-sensitive mutants (*dgt*) are characterized by impairments in the usage of starch that led to lower growth, most likely associated with decreased respiration. Collectively, our findings suggest that mutations in different components of the auxin signalling pathway specifically modulate photosynthetic and respiratory processes.

## KEYWORDS

auxin, metabolic adjustment, mitochondria, photosynthesis, plant hormones, respiration, stomata

## 1 | INTRODUCTION

Plant hormones relay information about internal and external conditions and thereby allow the maintenance of cell homeostasis. Auxin was first identified as a plant hormone on the basis of its ability to

stimulate differential growth in response to different stimuli (Davis, 2005). Auxin distribution within plant tissues controls an impressive variety of developmental processes (Vanneste & Friml, 2009). Although there are numerous chemical forms of auxin, the most abundant and physiologically relevant is indole-3-acetic acid (IAA; Enders &

Strader, 2015). Several processes are affected by IAA; among them are cell expansion, formation of floral organs, vascular tissue differentiation, apical dominance, side branching, and suppression of leaf abscission (Enders & Strader, 2015). Insights into auxin transport and signalling have allowed significant advances in elucidating its role in plant development. Manipulation of auxin signalling could be used to alter crop performance; however, its effects on primary metabolism remain largely unexplored (Leyser, 2017).

The auxin signalling pathway is mediated by a complex system of transcriptional regulators of the AUXIN/INDOLE ACETIC ACID (*Aux/IAA*) family (Delker, Raschke & Quint, 2008), controlling the interaction between auxin and its receptors including TRANSPORT INHIBITOR RESPONSE 1 (*TIR1*), which is a member of the AUXIN SIGNALING F-BOX PROTEIN (*AFB*) family (Leyser, 2017). Members of the *Aux/IAA* gene family have highly specific spatial and temporal expression patterns, thus contributing to the diversity of auxin responses in different plant, tissues, organs, and developmental stages (Audran-Delalande et al., 2012). For instance, downregulation of the tomato (*Solanum lycopersicum*) *Aux/IAA9* (*SlIAA9*, also known as *ENTIRE*) generates a constitutive auxin response associated to specific phenotypes, such as leaf morphogenesis, whereby the compound leaves of tomato are converted to simple leaves and the plants yield parthenocarpic fruits (Wang et al., 2005). By contrast, the tomato *diageotropica* (*dgt*) mutant is characterized by reduced sensitivity to auxin caused by loss of function in a cyclophilin A protein, with peptidyl-prolyl *trans-cis* isomerase (*PPase*) enzymatic activity (Oh, Ivanchenko, White, & Lomax, 2006). The *dgt* mutation leads to pleiotropic phenotypes, including impaired gravitropic response (Rice & Lomax, 2000), absence of lateral root branching (Muday, Lomax, & Rayle, 1995), reduced polar auxin transport and apical dominance (Ivanchenko et al., 2015), and altered vascular development (Zobel, 1973). Furthermore, *DGT* is essential in determining final fruit size, through the control of cell division and cell expansion (Devoghalare et al., 2012). In addition, the *dgt* mutation is also thought to disrupt a signalling cascade that includes the extracellular auxin binding protein 1 (*ABP1*; Christian, Steffens, Schenck, & Lüthen, 2003), a putative receptor for a non-canonical auxin signalling pathway. Interestingly, mutants of *dgt* orthologs have been discovered in the moss *Physcomitrella patens* (Lavy, Prigge, Tigyí, & Estelle, 2012) and in rice (*Oryza sativa*; Zheng et al., 2013). These mutants display similar phenotypes to tomato *dgt* plants and additionally exhibit altered auxin sensitivity. Molecular and biochemical studies seeking to understand the role of cyclophilins in the auxin response were performed by studying the *dgt* ortholog from rice, *LATERAL ROOTLESS 2* (*LRT2*; Jing et al., 2015). In brief, the authors demonstrated that *LRT2* can directly regulate the stability of *Aux/IAA* proteins, with *OsIAA11*, controlling the interaction between *TIR1* and IAA and affecting the life span of *Aux/IAA* proteins as a mechanism regulating auxin signalling.

Plant mitochondria play an essential and key role in the biosynthesis of adenosine triphosphate (ATP) through oxidative phosphorylation (Plaxton & Tran, 2011). Accordingly, the tricarboxylic acid (TCA) cycle in the mitochondria is fundamental in catalysing the oxidation of acetyl-CoA into CO<sub>2</sub>, simultaneously producing NADH, FADH<sub>2</sub>, ATP, and carbon skeletons used as substrates for several metabolic processes (Araújo, Nunes-Nesi, Nikoloski, Sweetlove, & Fernie, 2012; Fernie, Trethewey, Krotzky, & Willmitzer, 2004). These

compounds are essential to support plant growth and are of pivotal importance in responses to different environmental conditions (Berkowitz, De Clercq, Van Breusegem, & Whelan, 2016; Millar, Whelan, Soole, & Day, 2011). Recent compelling evidence has shown that plant hormones can regulate networks affecting mitochondrial metabolism (Berkowitz et al., 2016). Interestingly, it has previously been suggested that auxin regulates mitochondrial respiration to meet the increased energy demand for growing cells (Leonova, Gamburg, Vojnikov, & Varakina, 1985). Although the role of auxin in controlling plant growth and development is well established, our understanding on the connections between auxin and primary metabolism remains limited. Early findings have demonstrated that compounds that inhibit the TCA cycle and respiratory chain also inhibit auxin-induced growth (Thimann, 1977). Furthermore, connections between mitochondrial function and auxin during plant growth and in response to stress have been observed (Berkowitz et al., 2016; Ivanova et al., 2014).

Although the importance of auxin for sugar metabolism and development has been established in tomato fruits (Gao et al., 2016; Li et al., 2017; Sagar et al., 2013) and Chinese pear (*Pyrus ussuriensis*; Huang et al., 2014), the potential consequences of auxin signalling for metabolic aspects in leaves has not been investigated yet. Here, we analysed tomato mutants with either increased (*entire*) or reduced (*dgt*) auxin signalling. We therefore investigated how these mutations influence plant growth, photosynthesis, water use, and respiration. Our results demonstrate that *dgt* displayed a range of morphological and anatomical alterations as well as reduced photosynthetic capacity. By contrast, the *entire* mutant was characterized by changes in the levels of TCA cycle intermediates and nitrogen-related metabolites, indicating that both genes controlling auxin signalling alter developmental and metabolic programs in illuminated leaves.

## 2 | MATERIAL AND METHODS

### 2.1 | Plant material and growth conditions

Seeds of the tomato (*S. lycopersicum* cv. Micro-Tom) wild-type (WT) and near isogenic lines *dgt* and *entire* in the same genetic background (cv. Micro-Tom), obtained as described previously (Carvalho et al., 2011), were surface-sterilized with 5% sodium hypochlorite for 10 min and then washed with running distilled water and subsequently sowed in a tray with commercial substrate (Tropstrato HT®). The phenotypes of the *dgt* and *entire* individual mutants in the Micro-Tom background closely resemble those previously published for the same mutations in other tomato cultivars (Wang et al., 2005; Ivanchenko et al., 2015).

Seven days after germination (or following the appearance of the first true leaf), seedlings were transferred to 3.5-L pots containing the same commercial substrate supplemented with 5 g L<sup>-1</sup> 4:14:8 NPK. Plants were grown in a greenhouse located in Viçosa (20°45'S, 42°15'W, 650 m above sea level), south-eastern Brazil, with a minimum of 400-μmol photons m<sup>-2</sup> s<sup>-1</sup>. Plants were watered regularly and throughout the entire growth period were maintained under naturally fluctuating conditions of light intensity, temperature, and relative air humidity. The mutated alleles were confirmed through Sanger DNA sequencing in an ABI Prism 3100 platform using primers specific

for *DGT* (Solyc01g111170), 5'-GAGTCGCCGTTTTAGGCTTT-3' and 3'-GCAACACAACAACCAATTACG-5' and *ENTIRE* (Solyc04g076850), 5'-GTTGTCAAGTGTGTGACAGCC-3' and 3'-TGTCACCTTACACATAGGCCA-5'. The relative abundance of transcripts was confirmed by quantitative real-time PCR (qRT-PCR), using specific primer pairs for *DGT* and *ENTIRE*: Forward 5'-GAGTCGCCGTTTTAGGCTTT-3', Reverse 5'-GCAACACAACAACCAATTACG-3' and Forward 5'-GTTGTCAAGTGTGTGACAGCC-3', Reverse 5'-TGTCACCTTACACATAGGCCA-3', respectively (for details, see Table S4). All physiological, biochemical, and molecular parameters analysed in the experiments were performed on the third fully expanded source leaves from 4-week-old plants. Additionally, the experiment was repeated at least three times (even in different growth facilities) with similar phenotypes observed each time.

## 2.2 | Growth analyses

Growth parameters were determined in 4-week-old plants by measuring plant height, stem diameter, number of leaves, and specific leaf area (SLA). Leaf area was measured using a scanner (Hewlett Packard Scanjet G2410, Palo Alto, California, USA) and processing the resulting images on ImageJ (Schneider, Rasband, & Eliceiri, 2012). SLA was measured as described previously (Hunt, Causton, Shipley, & Askew, 2002). At the end of the experiment, plants were harvested by cutting the shoot 1 cm above ground level, thus separating shoots from roots. The roots, after water washing off soil contamination, and shoots were placed in labelled paper bags and brought to a forced air circulation oven at 70°C for 5 days; after which, the dry weight of roots and shoots (stem, petioles, and leaves) was determined in an electronic balance.

## 2.3 | Stomatal density, stomatal index, and leaf anatomy

After 2 hr under sunlight, leaf impressions were taken from the abaxial and adaxial surface of the third fully expanded leaf with dental resin imprints (Berger & Altmann, 2000). After shaping the leaf surfaces, nail polish copies were made using a colorless glaze (von Groll, Berger, & Altmann, 2002). The images were analysed under a light microscope (Olympus model AX70TRF; Olympus Optical, Tokyo, Japan) equipped with a U-Photo System and digital camera (AxioCam HRC; Zeiss, Göttingen, Germany). Stomatal density, stomatal index, and stomatal pore aperture were determined in at least 10 different fields of 0.10 mm<sup>2</sup> per leaf from at least seven different plants.

For leaf anatomy analyses, sections of the terminal leaflet of the third fully expanded leaf were hand cut from the widest part of the leaf using a razor blade and stored in 100% methanol for epidermal analysis, or in formaldehyde-acetic acid in ethanol 70% (v/v) solution for 24 hr for transverse analysis (Feder & O'Brien, 1968) and afterwards embedded in resin (historesin), sectioned in ~5-µm RM 2155 Automated Microtome, Leica. Sections were next mounted on a microscopy slide and stained with 1% (w/v) toluidine blue. Histological sections were observed under a light microscope (Olympus model AX70TRF; Olympus Optical, Tokyo, Japan) and images captured using a digital camera (AxioCam HRC; Zeiss, Göttingen, Germany). Images were analysed using ImageJ (Schneider et al., 2012).

## 2.4 | Water loss measurements

For water loss measurements, the weight of detached leaves, incubated with the abaxial side up under the same growth conditions described above, was determined over 4 hr at the indicated time points. Water loss was calculated as a percentage of the initial fresh weight (Araújo et al., 2011).

## 2.5 | Auxin sensitivity assays

In order to investigate root formation in response to auxin, an in vitro assay was performed using cotyledon explants taken from 8-day-old seedlings (after sowing) grown in culture medium. Five biological replicates composed by a Petri dish containing 20 explants were used for each treatment. The explants were kept for 10 days on Murashige-Skoog medium supplemented with vitamins B5 plus 30 g/L of sucrose, 6 g/L of agar, and 0.4 µM of NAA (α-naphthalene acetic acid—Sigma-Aldrich, St. Louis, MO, USA) at 25°C 16-hr day/8-hr night (Murashige & Skoog, 1962). The auxin response curve using hypocotyl segments was performed using 10-day-old seedlings (after sowing) grown under greenhouse conditions. The explants were collected using a razor blade (approximately 12 cm) and placed in Petri dishes containing Kelly and Bradford solution (Kelly and Bradford, 1986) added with different IAA concentrations. After 24 hr, hypocotyls were scanned at 300 dpi, and the generated images were captured using a digital camera (AxioCam HRC; Zeiss, Göttingen, Germany).

## 2.6 | Measurements of gas exchange and chlorophyll fluorescence

Gas exchange parameters were determined simultaneously with chlorophyll *a* (Chl *a*) fluorescence measurements as described in (Medeiros et al., 2016) using an open-flow infrared gas exchange analyser system (LI-6400XT; LI-COR Inc., Lincoln, NE) equipped with an integrated fluorescence chamber (LI-6400-40; LI-COR Inc.). Instantaneous gas exchanges were measured after 1-hr illumination during the light period under 1,000 µmol m<sup>-2</sup> s<sup>-1</sup> at the leaf level (light saturation) of photosynthetically active photon flux density (PPFD), determined by A/PPFD curves—net photosynthesis ( $A_N$ ) in response to PPFD curves (Figure S6 and Table S1). The reference CO<sub>2</sub> concentration was set at 400-µmol CO<sub>2</sub> mol<sup>-1</sup> air. All measurements were performed using the 2-cm<sup>2</sup> leaf chamber at 25°C, as well as a 0.5 stomatal ratio (amphistomatic leaves), and leaf-to-air vapour pressure deficit was kept at 1.2 kPa, and the amount of blue light was set to 10% PPFD to optimize stomatal aperture. Briefly, the initial fluorescence emission ( $F_0$ ) was by illuminating dark-adapted leaves (1 hr) with weak modulated measuring beams (0.03 µmol m<sup>-2</sup> s<sup>-1</sup>). A saturating white light pulse (8,000 µmol m<sup>-2</sup> s<sup>-1</sup>) was applied for 0.8 s to obtain the maximum fluorescence (Laskowski et al., 2008), from which the variable-to-maximum Chl fluorescence ratio was then calculated:  $F_v/F_m = [(F_m - F_0)/F_m]$ . In light-adapted leaves, the steady-state fluorescence yield was measured with the application of a saturating white light pulse (8,000 µmol m<sup>-2</sup> s<sup>-1</sup>) to achieve the light-adapted maximum fluorescence ( $F_m'$ ). A far-red illumination (2 µmol m<sup>-2</sup> s<sup>-1</sup>) was applied after turning off the actinic light to measure the light-adapted initial fluorescence ( $F_0'$ ). The capture efficiency of excitation

energy by open photosystem II reaction centers ( $F_v/F_m$ ) was estimated following Logan, Adams, and Demmig-Adams (2007) and the actual PSII photochemical efficiency ( $\phi_{PSII}$ ) was estimated as  $\phi_{PSII} = (F_m' - F_s)/F_m'$  (Genty, Briantais, & Baker, 1989).

According to Genty et al. (1989),  $\Phi_{PSII}$  represents the number of electrons transferred per photon absorbed in the PSII, the electron transport rate ( $J_{flu}$ ) was calculated as  $J_{flu} = \Phi_{PSII} \cdot \alpha \cdot \beta \cdot \text{PPFD}$ , where  $\alpha$  is leaf absorptance and reflects  $\beta$  the partitioning of absorbed quantum between and PSI and PSII. The product  $\alpha\beta$  was determined according with previous studies of optical properties using a double integrated ball system ISP-REF (OceanOptics, Inc., Dunedin, Florida, EUA), measuring the reflectance (R) and transmittance (T) and then calculating the absorbance (A), according with the followed equation:  $A = 1 - (R + T)$ . The  $\beta$  value was considered the standard fraction of quanta (0.5) and  $\alpha$  was 0.85, where 0.425 is the product already shown in Gilbert, Pou, Zwieniecki, and Holbrook (2012). Dark respiration ( $R_d$ ) was measured after 2 hr in the dark period (at night), using the same gas exchange system described above, and it was divided by two ( $R_d/2$ ) to estimate the mitochondrial respiration rate in the light ( $R_L$ ; Niinemets, Díaz-Espejo, Flexas, Galmés, & Warren, 2009).

Photosynthetic light-response curves ( $A/\text{PPFD}$ ) were determined using ambient  $\text{CO}_2$  concentration ( $C_a$ ) of  $400 \mu\text{mol CO}_2 \text{ mol}^{-1}$  and an initial PPFD of  $1,000 \mu\text{mol photon m}^{-2} \text{ s}^{-1}$ . PPFD was next increased to 1,200 and 1,400  $\mu\text{mol m}^{-2} \text{ s}^{-1}$  and thereafter decreased to 0  $\mu\text{mol m}^{-2} \text{ s}^{-1}$  (step changes to 1,000, 800, 400, 200, 100, 50, 25, 10, and 0  $\mu\text{mol m}^{-2} \text{ s}^{-1}$ ). Simultaneously, Chl *a* fluorescence parameters were obtained (Wong, Chen, Huang, & Weng, 2012). The responses of  $A_N$  to  $C_i$  ( $A/C_i$  curves) were initiated at saturating light of  $1,000 \mu\text{mol m}^{-2} \text{ s}^{-1}$  at  $25^\circ\text{C}$  under ambient  $\text{O}_2$  concentration (21%). Measurements were taken at ambient  $\text{CO}_2$  concentration ( $C_a$ ) of  $400 \mu\text{mol mol}^{-1}$ , and once the steady state was reached,  $C_a$  was decreased stepwise to  $50 \mu\text{mol mol}^{-1}$ . Upon completion of the measurements at low  $C_a$ ,  $C_a$  was returned to  $400 \mu\text{mol mol}^{-1}$  to restore the original  $A_N$ . Next,  $C_a$  was increased stepwise to  $1,600 \mu\text{mol mol}^{-1}$  in a total of 13 different  $C_a$  values (Long & Bernacchi, 2003). Following Rodeghiero, Niinemets, and Cescatti (2007), corrections were made for the leakage of  $\text{CO}_2$  into and water vapour out of the leaf chamber of the LI-6400 and were applied to all gas exchange data.  $A/C_i$  and  $A_N/\text{PPFD}$  curves were obtained using the third leaf, totally expanded.

## 2.7 | Determination of mesophyll conductance ( $g_m$ ), maximum rate of carboxylation ( $V_{cmax}$ ), maximum rate of carboxylation limited by electron transport ( $J_{max}$ ), and photosynthetic limitations

The  $\text{CO}_2$  concentration in the carboxylation sites ( $C_c$ ) was calculated according to (Harley, Loreto, Di Marco, & Sharkey, 1992) as

$$C_c = (\Gamma^* (J_{flu} + 8(A_N + R_L)) / (J_{flu} - 4(A_N + R_L))),$$

where the conservative value of  $\Gamma^*$  for tomato was taken from (Hermida-Carrera, Kapralov, & Galmés, 2016). Then  $g_m$  was estimated as the slope of the  $A_N$  vs  $C_i$ - $C_c$  relationship as  $g_m = A_N / (C_i - C_c)$ .

Thus,  $g_m$  was estimated based on average over the points used in the relationship ( $C_i < 300 \mu\text{mol mol}^{-1}$ ). Furthermore, the methods for estimating  $g_m$  include several assumptions as well as technical limitations, along with sources of error, which need to be considered to obtain reliable values (Pons et al., 2009).  $g_m$  was estimated according to the (Ethier & Livingston, 2004) method, which fits  $A_N/C_i$  curves with a nonrectangular hyperbola version of the Farquhar-von Caemmerer-Berry model, based on the hypothesis that  $g_m$  reduces the curvature of the Rubisco-limited portion of an  $A_N/C_i$  curve.

From  $A_N/C_i$  and  $A_N/C_c$  curves, the maximum carboxylation velocity ( $V_{cmax}$ ) and the maximum capacity for electron transport rate ( $J_{max}$ ) were calculated by fitting the mechanistic model of  $\text{CO}_2$  assimilation (Farquhar, von Caemmerer, & Berry, 1980), using the  $C_i$  and  $C_c$  based on temperature of kinetic parameters of Rubisco ( $K_c$  and  $K_o$ ), and  $V_{max}$ ,  $J_{max}$ , and  $g_m$  were normalized to  $25^\circ\text{C}$  using the temperature response and plug-in equations as previously described (Sharkey, Bernacchi, Farquhar, & Singaas, 2007)

The photosynthetic limitations were estimated as described previously (Grassi & Magnani, 2005). Briefly, this method uses the values of  $A_N$ ,  $g_s$ ,  $g_m$ ,  $V_{cmax}$ ,  $\Gamma^*$ ,  $C_c$ ,  $K_m$ , and  $K_m = K_c (1 + O/K_o)$  and permits the partitioning into the functional components of photosynthetic constraints related to stomatal ( $l_s$ ), mesophyll ( $l_m$ ), and biochemical ( $l_b$ ) limitations:

$$l_s = \frac{\left( \frac{g_{tot} \partial A_N}{g_s \partial C_c} \right)}{\left( g_{tot} + \frac{\partial A_N}{\partial C_c} \right)}$$

$$l_m = \frac{\left( \frac{g_{tot} \times \partial A_N}{g_m \times \partial C_c} \right)}{g_{tot} + \left( \frac{\partial A_N}{\partial C_c} \right)}$$

$$l_b = \frac{g_{tot}}{\left( g_{tot} + \partial A_N / \partial C_c \right)},$$

$g_{tot}$  is the total conductance to  $\text{CO}_2$  from ambient air to chloroplasts: ( $g_{tot} = 1 / [(1/g_s) + (1/g_m)]$ ). The fraction  $\partial A_N / \partial C_c$  was calculated as

$$\frac{\partial A_N}{\partial C_c} = \frac{\left( \left[ V_{cmax} (\Gamma^* + K_m) \right] \right)}{(C_c + K_m)^2}$$

## 2.8 | Determination of metabolite levels

Leaf samples were harvested in different time points along the light/dark cycle (0, 3, 6, 9, 12, 15, 18, 19, 21, and 24 hr), immediately frozen in liquid nitrogen and stored at  $-80^\circ\text{C}$  until further analysis. The extraction was performed by rapid grinding of tissue in liquid nitrogen and immediate addition of the appropriate extraction buffer. The levels of starch, sucrose, fructose, and glucose in the leaf tissue were determined exactly as described previously (Ferne, Roscher, Ratcliffe, & Kruger, 2001). Photosynthetic pigments were determined according to the methods described by Porra, Thompson, and Kriedemann



(1989). Malate and fumarate were determined according to Nunes-Nesi et al. (2007). Proteins and amino acids were also determined as described previously (Gibon et al., 2004). The metabolites profile was carried out in samples harvested at the middle of the day (Liseč, Schauer, Kopka, Willmitzer, & Fernie, 2006). The extraction was performed using 1 ml of methanol and shaking (800 rpm) at 70°C during 15 min; 60 µl of Ribitol (0.2 mg ml<sup>-1</sup>) was added as an internal standard. After that, the derivatization procedure was performed exactly as described in Roessner et al. (2001). Peaks were manually annotated, and ion intensity was determined by the aid of TagFinder software (Luedemann, von Malotky, Erban, & Kopka, 2011), using a reference library from the Golm Metabolome Database (Kopka et al., 2004) and following the recommended reporting format (Fernie et al., 2011).

## 2.9 | Measurement of respiratory parameters based on <sup>14</sup>CO<sub>2</sub> evolution

Estimation of the TCA cycle flux was calculated on the basis of <sup>14</sup>CO<sub>2</sub> evolution (Nunes-Nesi et al., 2005). The experiment was carried out following incubation of isolated leaf discs in 10-mM 2-(N-morpholine)-ethanesulphonic acid (MES)-KOH, pH 6.5, containing 0.3-mM glucose (Glc) and supplied with 0.62 KBq ml<sup>-1</sup> of [1-<sup>14</sup>C]- or [3,4-<sup>14</sup>C] Glc under 150-µmol photons m<sup>-2</sup> s<sup>-1</sup> light. Evolved <sup>14</sup>CO<sub>2</sub> was trapped in KOH and quantified by liquid scintillation counting. The fractionation of <sup>14</sup>C-labelled material was performed exactly as detailed previously (Lytovchenko, Sweetlove, Pauly, & Fernie, 2002). The results were interpreted following recommendations of ap Rees and Beevers (1960).

## 2.10 | Expression analysis by qRT-PCR

qRT-PCR analysis was performed exactly as described by Zanor et al. (2009) with total RNA isolated from at least three biological replicates. The samples were harvested and snap frozen in liquid nitrogen. RNA extraction was performed using TRIzol® reagent (Ambion, Life Technology) following the manufacturer's manual. Digestion with DNase I (Ambion; <http://www.ambion.com/>) was performed according to the manufacturer's instructions. The integrity of the RNA was checked on 1% (w/v) agarose gels, and the concentration was measured before and after DNase I digestion using a Nanodrop ND-1000 spectrophotometer (<http://www.nanodrop.com/>). DNA was synthesized from 1 µg of total RNA using SuperScript III reverse transcriptase (Invitrogen; <http://www.invitrogen.com/>) according to the manufacturer's instructions. The efficiency of cDNA synthesis was estimated by semi-quantitative PCR using two primer pairs amplifying 5' and 3' regions of the constitutive gene Actin (forward [5'-GGTCCCTCTATTGTCCACAG-3'] and reverse [5'-TGCATCTCTGGTCCAGTAGGA-3']). Gene expression values were normalized based on the Actin (Solyc03g078400.2.1) gene with the following primers, forward (5'-GGTCCCTCTATTGTCCACAG-3') and reverse (5'-TGCATCTCTGGTCCAGTAGGA-3'). The primers used for qRT-PCR were designed using the QuantiPrime software (<http://www.quantprime.de>). Detailed primers information is described in the Table S7.

## 2.11 | Experimental design and statistical analysis

The experiments were arranged in a completely randomized design. All data passed the normality and equal variance Kolmogorov–Smirnov tests and then the means were further analysed by a one-way analysis of variance and some cases in two-way, when necessary. The means separations were further performed by multiple comparison using a most rigorous test in comparative statistics, the Tukey test ( $P < 0.05$ ). The means  $\pm$  SE presented in the tables and figures were obtained from seven independent replicates per genotype and when was the case, over time.

## 3 | RESULTS

### 3.1 | *Diageotropica* mutation reduces plant growth and intrinsic water-use efficiency

Here, we investigated the physiological and metabolic impacts of fluctuations on auxin signalling using previously characterized tomato mutants with either increased (*entire*, a mutation in the *SIIAA9* gene) or reduced (*dgt*) auxin signalling. The mutants show a clearly distinct phenotype during vegetative growth (Figure 1a and Table 1). In an attempt to show this differential sensitivity of auxin, we initially confirmed that *SIIAA9* and *DGT* expression were significantly reduced in *entire* and *dgt* mutant plants, respectively (Figure 1b). Furthermore, the expression of *DGT* in the *entire* mutant and of *SIIAA9* in the *dgt* mutant did not differ significantly compared to WT control plants (Figure 1b). We next evaluated the expression levels of the *DGT* and *SIIAA9* genes in different tissues of WT plants. Our results showed that the basal expression of both genes is highly variable across the whole plant. Thus, while *DGT* is highly expressed in roots, young leaves, mature leaves, and open flowers, *SIIAA9* is expressed in young leaves, mature leaves, flowers, and young fruits (Figure S1). Our results are in good agreement with both previously published results (Wang et al., 2009) and public RNA-Seq data in tomato cv. Micro-Tom plants (<http://tomexpress.toulouse.inra.fr/select-data>).

In order to confirm the alteration in the auxin sensitivity in *dgt* and *entire* plants, we next investigated the auxin dose effect on both root formation and hypocotyl segment elongation (Figure S2). The *entire* mutant plants do not present a significant increase in auxin sensitivity when compared with WT although it does respond differentially to exogenously applied auxin; moreover, *entire* presents a significantly increased sensitivity in comparison with *dgt* mutant. Thus, at 0.5 µM of NAA, 90% of explants from *entire* plants displayed regenerated roots, while only 60% of the total in *dgt* explants regenerated. In summary, *dgt* plants displayed reduced sensitivity to auxin, characterized by reduced root production in explants (Figure S2A,B) as well as failure of hypocotyls to elongate (Figure S2C).

In an attempt to show the effect of changes in auxin signalling, we decided to analyse whole plant traits of both mutants. The *entire* plants were characterized by increased number of leaves and total dry weight, but thinner leaves with reduced SLA and stomatal density (Table 1 and Figure S3). Although such leaf phenotypes could

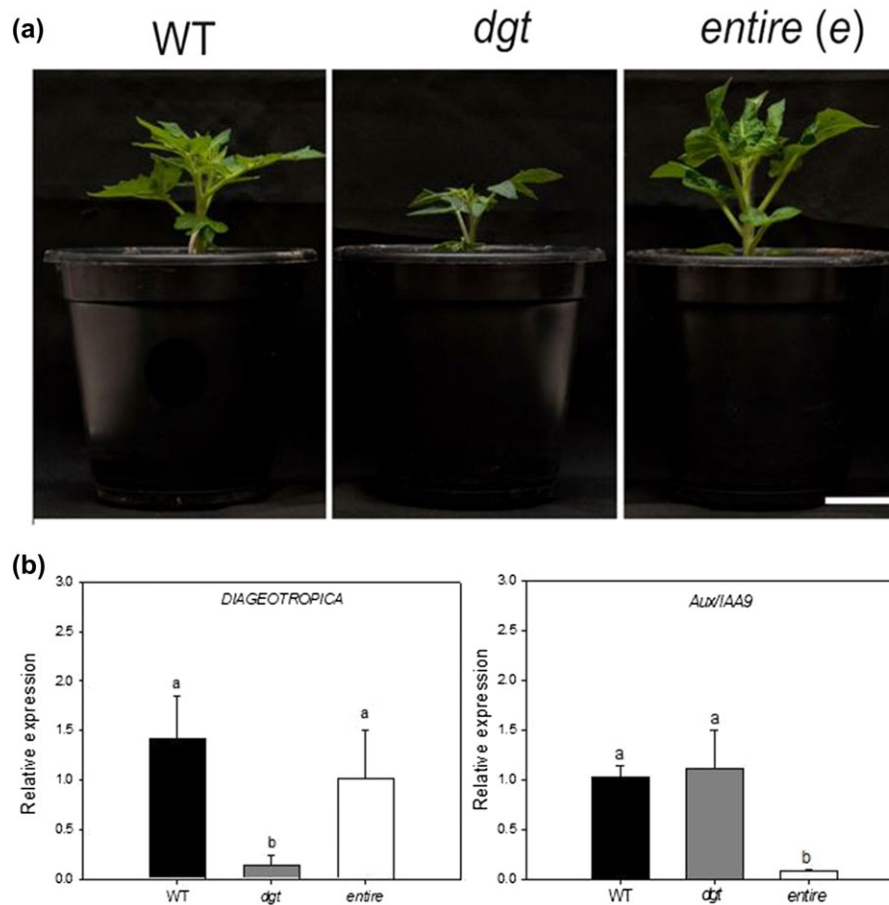


**FIGURE 1** Phenotypic and molecular characterization of auxin signalling mutants. (a) Representative images of 4-week-old plants with either increased (*entire*) or reduced (*diageotropica*, *dgt*) auxin signalling, compared with wild-type (WT, tomato cv. Micro-Tom) plants growing under optimal conditions. (b) Relative transcript expression performed by quantitative real-time PCR (qRT-PCR) showed significant reduction in the expression of mutant alleles, with no effect on the wild-type alleles. Data are normalized with respect to the average response calculated for the corresponding WT. WT, black bars; *dgt*, grey bars, *entire*, white bars. Data are means  $\pm$  SE ( $n = 5$ ). Different letters represent average values that were judged to be statistically different between genotypes ( $P < 0.05$ , Tukey test) [Colour figure can be viewed at [wileyonlinelibrary.com](http://wileyonlinelibrary.com)]

**TABLE 1** Growth and morphology of wild-type and auxin signalling related mutants

Parameters	WT	<i>dgt</i>	<i>entire</i>
Plant height (cm)	6.1 $\pm$ 0.2 a	4.9 $\pm$ 0.2 b	6.6 $\pm$ 0.4 a
Total leaf area (cm <sup>2</sup> )	47.0 $\pm$ 3.7 a	21.5 $\pm$ 1.9 b	43.8 $\pm$ 2.6 a
SLA (cm <sup>2</sup> g <sup>-1</sup> )	177.6 $\pm$ 9.3 b	254.2 $\pm$ 17.2 a	133.7 $\pm$ 1.5 c
TDW (g)	0.29 $\pm$ 0.02 b	0.13 $\pm$ 0.01 c	0.41 $\pm$ 0.02 a
Abaxial stomatal density (mm <sup>2</sup> )	165.76 $\pm$ 10.2 a	155.54 $\pm$ 4.7 a	91.07 $\pm$ 2.9 b
Adaxial stomatal density (mm <sup>2</sup> )	40.79 $\pm$ 2.89 a	37.07 $\pm$ 2.1 a	32.48 $\pm$ 2.2 b
Abaxial stomatal index (%)	50.22 $\pm$ 2.39 a	12.73 $\pm$ 0.5 c	47.55 $\pm$ 3.1 a
Adaxial stomatal index (%)	10.84 $\pm$ 2.16 a	14.05 $\pm$ 2.4 a	15.52 $\pm$ 0.8 a
Abaxial pore area ( $\mu$ m <sup>2</sup> )	120.59 $\pm$ 0.87 b	105.62 $\pm$ 5.6 c	194.95 $\pm$ 8.6 a
Adaxial pore area ( $\mu$ m <sup>2</sup> )	103.93 $\pm$ 2.52 b	57.28 $\pm$ 2.0 c	134.33 $\pm$ 2.3 a
Leaf thickness ( $\mu$ m)	80.89 $\pm$ 8.45 b	105.4 $\pm$ 14.8 a	48.98 $\pm$ 9.6 c
RWC (%)	82.61 $\pm$ 1.38 a	80.97 $\pm$ 0.58 a	85.53 $\pm$ 1.2 a

*Note.* Plants with either increased (*entire*) or reduced (*diageotropica*, *dgt*) auxin signalling were compared with wild-type (WT) plants growing under optimal conditions. Data presented are mean  $\pm$  SE ( $n = 7$ ) obtained in at least two independent assays. Different letters represent average values that were judged to be statistically different between genotypes ( $P < 0.05$ , Tukey test). SLA: Specific leaf area; TDW: total dry weight; RWC: relative water content.

potentially affect water relations, relative water content was invariant between WT and mutant plants (Table 1). Moreover, as shown in Table 1, *dgt* plants exhibited higher SLA and leaf thickness in

comparison with the other genotypes. Additionally, *dgt* has significantly reduced plant height as well as total leaf area, followed by reduced total dry weight. Leaf morphology was also changed in

*dgt* plants, as observed by their reduced stomatal index and stomatal pore diameters (Figures S3 and S4). These morphological alterations culminated with changes in water use as demonstrated by enhanced water loss in detached leaves of *entire*, whereas in *dgt*, water loss was decreased, in comparison with WT (Figure S5 and Table S1).

### 3.2 | The *entire* and *diageotropica* mutations alter the expression profile of AUXIN RESPONSE FACTORS and AUXIN/INDOLE-3-ACETIC ACID INDUCIBLE genes

Auxin is considered a potent regulator of several aspects of plant function, and this response is dependent on several genes whose expression is upregulated in response to its application (Quint & Gray, 2006). Among the most thoroughly characterized gene families are SAURs (Small Auxin-Up RNAs), GH3s (*Gretchen Hagen 3*), and *Aux/IAAs* (*Auxin/INDOLE ACETIC ACID INDUCED*) gene families, which are induced within minutes of auxin application (Hedden & Thomas, 2008). These genes products, as well as the auxin response factors (ARFs), likely confer specificity to the auxin response through regulation of other transcription factors and effector genes (Leyser, 2017). We therefore investigated the expression levels of genes involved in auxin signalling, including *IAA1*, *IAA2*, *IAA3*, *ENTIRE/IAA9*, *IAA19*, *IAA29*, *ARF8*, *ARF10*, *DGT*, and *GH3*, and observed that both gene families (*Aux/IAAs* and *ARFs*) are differentially expressed in response to changes in auxin signalling (Figure 2). Transcript analysis revealed that *ARF* (*ARF8* and *ARF10*), as well as *IAA19* and *IAA29* expression, is upregulated in *dgt* mutant (Figure 2). In the *entire* mutant, the levels of *IAA1*, *IAA2*, *IAA3*, *IAA19*, *IAA29*, and *GH3* were upregulated in comparison with WT; however, no differences were observed in the expression of *IAA3*, *IAA19*, and *IAA29* between mutant lines. Our results suggest that the *DGT* gene regulates the expression of members of the *ARFs* and *Aux/IAAs* families, whereas *SIIAA9* (*ENTIRE*) can regulate genes of its own family (*AUX/IAAs*), as well as member of the *GH3* family (Figure 2).

### 3.3 | The *entire* mutation improves photosynthetic capacity by reducing stomatal resistance

Given the alterations observed in morphology and growth, we next performed a full characterization of the photosynthetic capacity of *dgt* and *entire* mutants. In close agreement with the stomatal density and stomatal index (Table 1), a significant reduction of net photosynthesis ( $A_N$ ), stomatal conductance ( $g_s$ ), and transpiration ( $E$ ) rates (12.5%, 28.5%, and 32.1% lower than WT values, respectively) was observed in *dgt* plants (Table 2). By contrast, significant increases in  $A_N$ ,  $g_s$ , and  $E$  (10.42%, 21%, and 12.5% of that of WT, respectively) were observed in *entire* plants (Table 2). The *dgt* mutant further displays higher intrinsic water-use efficiency ( $WUE_i$ ) than WT and *entire* plants. Lower  $WUE_i$  in *entire* plants is in agreement with stomatal pore area (Table 2 and Figures S3 and S5). The higher  $CO_2$  uptake capacity observed in *entire* was coupled with higher  $R_d$  (Table 2), significantly higher than WT and *dgt* (nearly two-fold in both cases). Despite these changes, no significant alterations in photorespiration ( $P_R$ ), maximum PSII photochemical efficiency ( $F_v'/F_m'$ ), actual PSII photochemical

efficiency ( $F_v'/F_m'$ ), and the electron transport rate ( $J_{flu}$ ) were found among the genotypes (Table 2). Photosynthetic light response curves revealed that mutants have altered  $A_N$  at high PPFD. The light-saturated  $A_N$  ( $A_{PPFD}$ ), light saturation ( $I_s$ ), and light compensation ( $I_c$ ) points were significantly higher in *entire* plants, whereas only  $I_s$  was reduced in *dgt* plants with no alterations in light-use efficiency ( $1/\phi$ ; Table S2 and Figure S6).

The response of  $A_N$  to leaf internal  $CO_2$  concentration ( $A_N/C_i$  curves; Figure 3a) was also obtained and subsequently converted into responses of  $A_N$  to chloroplastic  $CO_2$  concentration ( $A_N/C_c$  curves; Figure 3b). Essentially, both  $A_N/C_i$  and  $A_N/C_c$  curves were similar regardless of genotype (Figure 3). Under ambient  $CO_2$  concentration ( $400 \mu\text{mol mol}^{-1}$ ),  $C_i$  and  $C_c$  estimations were lower in *dgt* and higher in *entire* plants compared with the WT (Table 3).  $g_m$  estimated using a combination of gas exchange and chlorophyll *a* fluorescence parameters via two independent methods did not show any significant difference between genotypes (Table 3). Considering that  $g_m$ , as well as  $R_L$ , changes dynamically under different environmental conditions, we performed a sensitivity curve response of  $g_m$  under different  $R_L$  (Figure S7). This analysis was performed considering different percentages of  $R_L$  (100%, 75%, 50%, 25%, and 0%) and following the expected changes in  $g_m$  (Figure S7). Our results showed no significant changes in  $g_m$  despite alterations in  $R_L$  even when 100% of  $R_L$  was considered in relation to  $R_d$  (1.51, 1.37, and  $2.70 \mu\text{mol CO}_2 \text{ m}^{-2} \text{ s}^{-1}$  in WT, *dgt*, and *entire*, respectively). As shown in Table 3, the maximum carboxylation velocity ( $V_{cmax\_cc}$ ) and maximum capacity for electron transport rate ( $J_{max\_cc}$ ) were similar between *dgt* and WT plants. On the other hand, reduced  $V_{cmax\_ci}$  and increased  $V_{cmax\_cc}$  without impacting either  $J_{max\_ci}:V_{cmax\_ci}$  or  $J_{max\_cc}:V_{cmax}$  were found in *entire* mutant plants (Table 3). Moreover, the similarities in the  $J_{max}:V_{cmax}$  ratios suggest that although differences in  $A_N$  were observed, an adequate functional balance between carboxylation and electron transport rates probably occurred despite changes in auxin signalling.

The overall photosynthetic limitations were next partitioned into their functional components, namely, stomatal ( $I_s$ ), mesophyll ( $I_m$ ), and biochemical ( $I_b$ ) limitations (Table 3). The photosynthetic rates were mainly constrained by  $I_b$  of around 50% in WT, whereas  $I_s$  accounted for, on average, 28% and 24% and  $I_m$  contributed 22% and 26% in WT and *entire* plants, respectively. Remarkably,  $I_b$  was reduced to about 40% and followed by increased  $I_s$  to around 38%, whereas  $I_m$  contributed 22% in *dgt* plants. These analyses demonstrated that auxin signalling-related mutants are affected mainly in  $I_s$ , in agreement with morphological alterations, particularly in *dgt* plants. Our results support the findings that variations in  $A_N$ , as described in Tables 2 and 3, should be primarily associated with stomatal conductance. Therefore, manipulation of auxin signalling could provide an effective means to alter maximum photosynthetic rate and hence productivity.

### 3.4 | DGT and ENTIRE integrate auxin signalling and growth by modulating plant energy status

To further explore the consequences of changes in the auxin signalling mutants, we conducted a detailed metabolic analysis in leaves. To this end, we first measured the levels of starch, soluble sugars (glucose, fructose, and sucrose), amino acids, and the organic acids, malate,

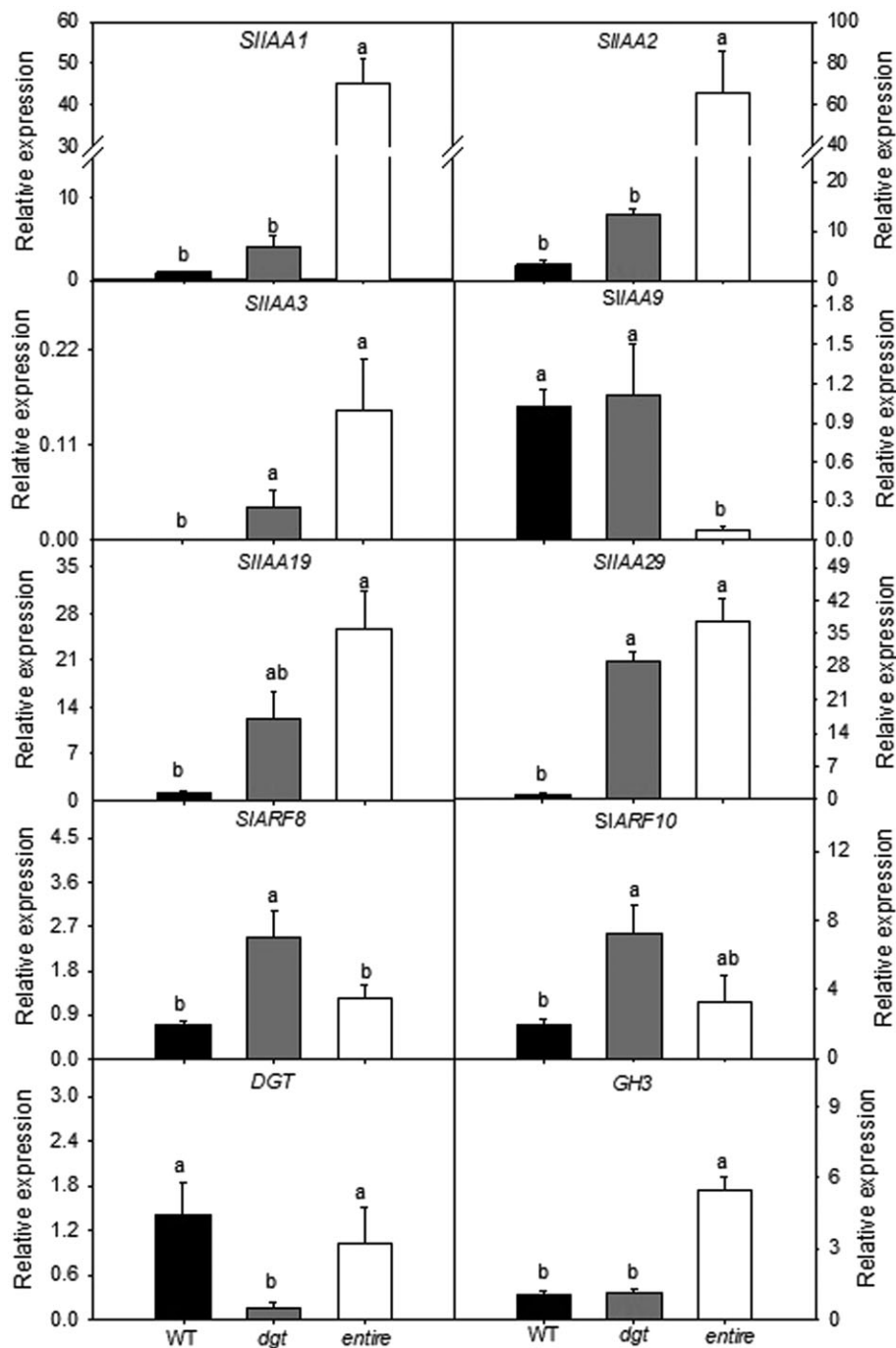


**FIGURE 2** Relative transcript accumulation of members of *SIIAA* and *SIARF* family genes is affected in auxin signalling mutants. Relative expression levels of genes involved in auxin signalling (*SIIAA* and *SIARF* family genes) and homeostasis (*GH3*) are altered in tomato plants with either increased (*entire*) or reduced (diageotropica, *dgt*) auxin signalling when compared with wild-type (WT) plants growing under optimal conditions. The y-axis values represent the relative expression levels calculated using the  $2^{-\Delta\Delta CT}$  method. Expression levels were normalized using actin and ubiquitin3 as reference. Values are presented as means  $\pm$  SE ( $n = 4$ ) of independent biological replicates. Different letters represent average values that were judged to be statistically different between genotypes ( $P < 0.05$ , Tukey test)

and fumarate during a diel cycle. Briefly, this analysis revealed that *dgt* plants were characterized by a significant increase in the levels of glucose, fructose, sucrose, and fumarate during the light period, but with no changes in malate and starch (Figure 4 and Table S3). Overall, plants with higher auxin sensitivity (*entire*) did not show significant changes in carbohydrate and organic acid levels during the diurnal cycle in comparison with WT plants (Figure 4 and Table S3). Interestingly, during the night, the usage of these accumulated metabolites in

*dgt* plants is not increased, and at the end of dark period, higher levels were observed (Figure 4). Notably, starch metabolism seems to be highly affected in *dgt* plants, particularly during the night, significantly higher in comparison with WT and *entire* mainly from 9:00 pm until 3:00 am; however, at the beginning of the day, no differences between genotypes were observed (Figure 4f and Table S3). In addition, the level of amino acids was significantly higher in leaves of *entire* plants when compared with both WT and *dgt*; however, in roots, it



**TABLE 2** Gas exchange and chlorophyll *a* fluorescence parameters are affected in auxin signalling related mutants

Parameters*	WT	dgt	entire
$A_N$ ( $\mu\text{mol CO}_2 \text{ m}^{-2} \text{ s}^{-1}$ )	19.17 $\pm$ 0.62 b	16.78 $\pm$ 0.30 c	21.18 $\pm$ 0.31 a
$g_s$ ( $\text{mol H}_2\text{O m}^{-2} \text{ s}^{-1}$ )	0.28 $\pm$ 0.01 b	0.20 $\pm$ 0.008 c	0.34 $\pm$ 0.018 a
$E$ ( $\text{mmol H}_2\text{O m}^{-2} \text{ s}^{-1}$ )	3.68 $\pm$ 0.26 b	2.50 $\pm$ 0.22 c	4.64 $\pm$ 0.28 a
$WUE_i$ (A/ $g_s$ )	69.32 $\pm$ 1.80 b	83.01 $\pm$ 4.04 a	61.89 $\pm$ 1.93 c
$R_d$ ( $\mu\text{mol CO}_2 \text{ m}^{-2} \text{ s}^{-1}$ )	1.43 $\pm$ 0.05 b	1.25 $\pm$ 0.11 b	2.94 $\pm$ 0.14 a
$P_R$ ( $\mu\text{mol CO}_2 \text{ m}^{-2} \text{ s}^{-1}$ )	3.69 $\pm$ 0.18 a	3.79 $\pm$ 0.29 a	3.66 $\pm$ 0.21 a
$F_v/F_m$	0.84 $\pm$ 0.001 a	0.84 $\pm$ 0.001 a	0.83 $\pm$ 0.001 a
$F_v'/F_m'$	0.59 $\pm$ 0.01 a	0.59 $\pm$ 0.011 a	0.61 $\pm$ 0.012 a
$J_{\text{flu}}$ ( $\mu\text{mol m}^{-2} \text{ s}^{-1}$ )	170.75 $\pm$ 3.71 a	161.54 $\pm$ 8.24 a	160.63 $\pm$ 4.92 a

Note. Data were obtained in 4-week-old plants with either increased (*entire*) or reduced (*diageotropica*, *dgt*) auxin signalling and were compared with wild-type (WT) plants growing under optimal conditions. Values are presented as means  $\pm$  SE ( $n = 7$ ). Different letters represent average values that were judged to be statistically different between genotypes ( $P < 0.05$ , Tukey test).

\* $A_N$ : Net photosynthesis rate;  $g_s$ : stomatal conductance;  $E$ : transpiration rate;  $WUE_i$ : intrinsic water-use efficiency;  $R_d$ : dark respiration;  $P_R$ : photorespiration rate;  $F_v/F_m$ : maximum PSII photochemical efficiency;  $F_v'/F_m'$ : actual PSII photochemical efficiency;  $J_{\text{flu}}$ : electron transport rate estimated by chlorophyll fluorescence parameters.

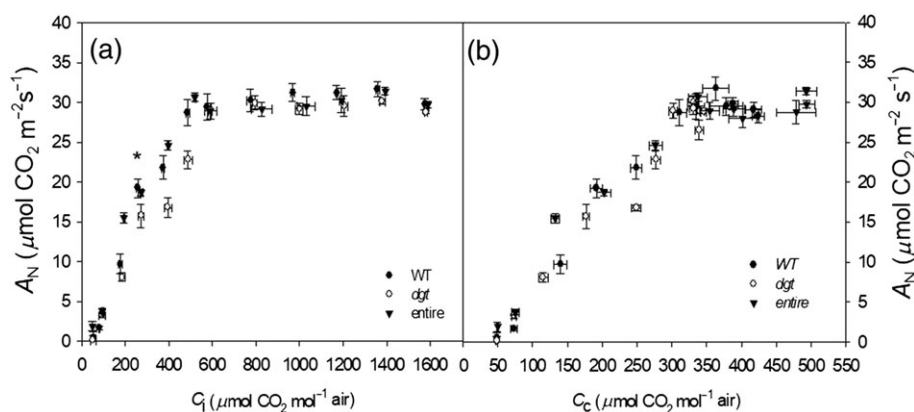


**FIGURE 3** Net photosynthesis ( $A_N$ ) curves in response to sub-stomatal ( $C_i$ ) or chloroplastic ( $C_c$ )  $\text{CO}_2$  concentration in auxin signalling mutants (*dgt* and *entire*). A,  $A_N/C_i$  curve, and B,  $A_N/C_c$ . Plants with either increased (*entire*) or reduced (*diageotropica*, *dgt*) auxin signalling were compared with wild-type (WT) plants growing under optimal conditions. WT, black circles; *dgt*, open circles; *entire*, black triangles. Data are means  $\pm$  SE ( $n = 7$ ) obtained using the third fully expanded leaf from the apex of 4-week-old plants (vegetative stage)

**TABLE 3** Photosynthetic characterization of auxin signalling mutants

Parameters*	WT	dgt	entire
$C_i$ ( $\mu\text{mol CO}_2 \text{ mol}^{-1}$ )	276.32 $\pm$ 15.71 b	208.82 $\pm$ 19.78 c	333.31 $\pm$ 17.49 a
$C_c$ ( $\mu\text{mol CO}_2 \text{ mol}^{-1}$ )	163.88 $\pm$ 9.75 a	117.05 $\pm$ 7.97 b	147.89 $\pm$ 8.90 a
$g_{m\_Harley}$ ( $\text{mol CO}_2 \text{ m}^{-2} \text{ s}^{-1} \text{ bar}$ )	0.215 $\pm$ 0.01 a	0.232 $\pm$ 0.024 a	0.211 $\pm$ 0.015 a
$g_{m\_Ethier}$ ( $\text{mol CO}_2 \text{ m}^{-2} \text{ s}^{-1} \text{ bar}$ )	0.234 $\pm$ 0.03 a	0.244 $\pm$ 0.056 a	0.224 $\pm$ 0.034 a
$V_{\text{cmax\_}C_i}$ ( $\mu\text{mol m}^{-2} \text{ s}^{-1}$ )	66.92 $\pm$ 3.30 a	69.362 $\pm$ 2.838 a	55.744 $\pm$ 3.051 b
$V_{\text{cmax\_}C_c}$ ( $\mu\text{mol m}^{-2} \text{ s}^{-1}$ )	107.307 $\pm$ 2.42 b	108.56 $\pm$ 1.83 b	121.95 $\pm$ 1.32 a
$J_{\text{max\_}C_i}$ ( $\mu\text{mol m}^{-2} \text{ s}^{-1}$ )	112.85 $\pm$ 6.97 a	112.68 $\pm$ 6.15 a	106.17 $\pm$ 6.45 a
$J_{\text{max\_}C_c}$ ( $\mu\text{mol m}^{-2} \text{ s}^{-1}$ )	134.40 $\pm$ 2.69	142.35 $\pm$ 6.81 a	148.88 $\pm$ 1.56 a
$J_{\text{max\_}C_i} : V_{\text{cmax\_}C_i}$	1.69 $\pm$ 0.11 a	1.62 $\pm$ 0.05 a	1.91 $\pm$ 0.10 a
$J_{\text{max\_}C_c} : V_{\text{cmax\_}C_c}$	1.25 $\pm$ 0.04 a	1.31 $\pm$ 0.07 a	1.22 $\pm$ 0.02 a
Stomatal limitation ( $I_s$ )	0.281 $\pm$ 0.015 a	0.381 $\pm$ 0.018 b	0.241 $\pm$ 0.007 a
Mesophyll limitation ( $I_m$ )	0.229 $\pm$ 0.011 a	0.224 $\pm$ 0.018 a	0.258 $\pm$ 0.004 a
Biochemical limitation ( $I_b$ )	0.493 $\pm$ 0.022 a	0.395 $\pm$ 0.012 b	0.501 $\pm$ 0.061 a

Note. Data were obtained in 4-week-old plants with either increased (*entire*) or reduced (*diageotropica*, *dgt*) auxin signalling and were compared with wild-type (WT) plants growing under 400  $\mu\text{mol CO}_2$  and 21%  $\text{O}_2$  and 1000 PAR. Values are presented as means  $\pm$  SE ( $n = 7$ ). Different letters represent average values that were judged to be statistically different between genotypes ( $P < 0.05$ , Tukey test).

\* $C_i$ : sub-stomatal  $\text{CO}_2$  concentration;  $C_c$ : Chloroplastic  $\text{CO}_2$  concentration;  $g_m$ : mesophyll conductance to  $\text{CO}_2$  estimated according to the Harley and Ethier;  $V_{\text{cmax\_}C_i}$  or  $C_c$ : maximum carboxylation capacity based on  $C_i$  or  $C_c$ ;  $J_{\text{max\_}C_i}$  or  $C_c$ : maximum capacity for electron transport rate based on  $C_i$  or  $C_c$ .

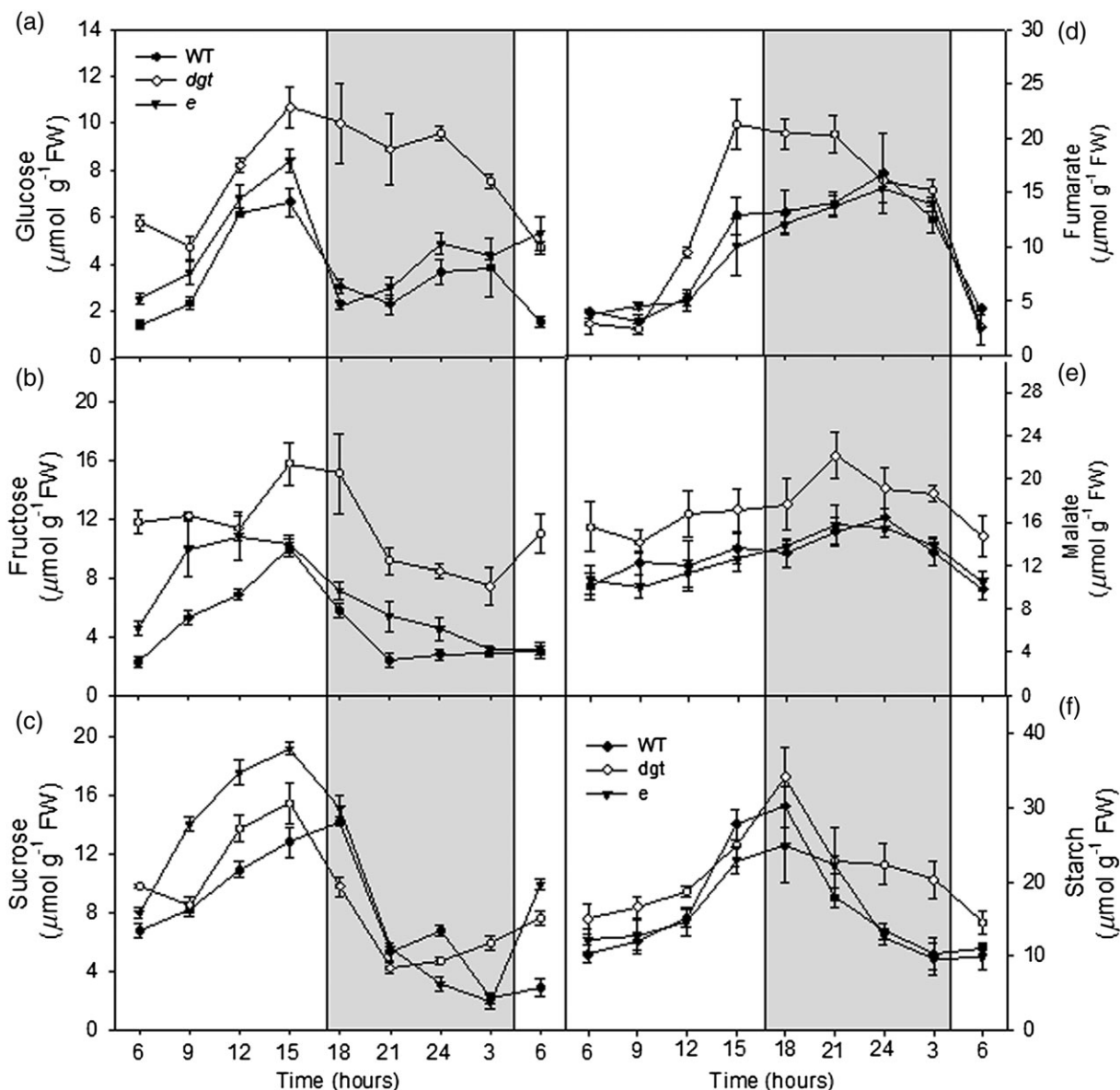


**FIGURE 4** Leaf metabolite levels are altered in auxin signalling mutants during the diurnal cycle. Diurnal changes in key metabolite content in leaves of tomato plants with either increased (*entire*) or reduced (*diageotropica*, *dgt*) auxin signalling were compared with wild-type (WT) plants growing under optimal conditions. (a) Glucose, (b) Fructose, (c) Sucrose; (d) Fumarate, (e) Malate, and (f) Starch levels were measured along a diurnal cycle. Samples were taken from the third fully expanded leaf from the apex of 4-week-old plants (vegetative stage) harvested every 3 hr along the diurnal cycle. WT, black circle; *dgt*, open circle and *entire*, black triangles. Data are means  $\pm$  SE ( $n = 6$ ). Grey bars indicate the dark period; white bars indicate the light period. FW: Fresh weight

was significantly higher in *entire* only in comparison with WT plants (Figure S8). Total protein content did not show any differences between genotypes. Nitrate concentration was greatly reduced in leaves of *dgt* plants, nearly 35% less in comparison with WT and *entire* mutant, without changes in roots (Figure S8). The *dgt* mutant also exhibited increased levels of carotenoids and chlorophyll *b* (Figure S9E-B).

We further extended this metabolic study to measure the levels of the intermediates of the primary plant metabolism by using an established gas chromatography–mass spectrometry (GC-MS) protocol for metabolic profiling (Lisec et al., 2006). This analysis revealed that among the 46 successfully annotated compounds related to primary metabolism, most of them displayed altered levels (Figure 5

and Table S5). Namely, considerable changes in the levels of a wide range of amino acids, organic acids, and sugars were observed (Figure 5; the full dataset is additionally provided as Table S5). Specifically, *entire* plants were characterized by increases in the levels of 10 amino acids, namely,  $\beta$ -alanine, arginine, asparagine, glutamine, lysine, methionine, ornithine, serine, threonine, and valine (Figure 5 and Table S5). Similarly, in *dgt* mutant plants, 10 of the individual amino acids were significantly increased, namely,  $\beta$ -alanine, GABA, glutamate, glycine, isoleucine, histidine, phenylalanine, proline, and tryptophan (Figure 5 and Table S5). Interestingly, some organic acids detected here have contrasting behaviour between the *dgt* and *entire* mutants including citrate, 2-oxoglutarate, succinate, fumarate, and malate, which were all increased in *dgt* plants but drastically decreased in

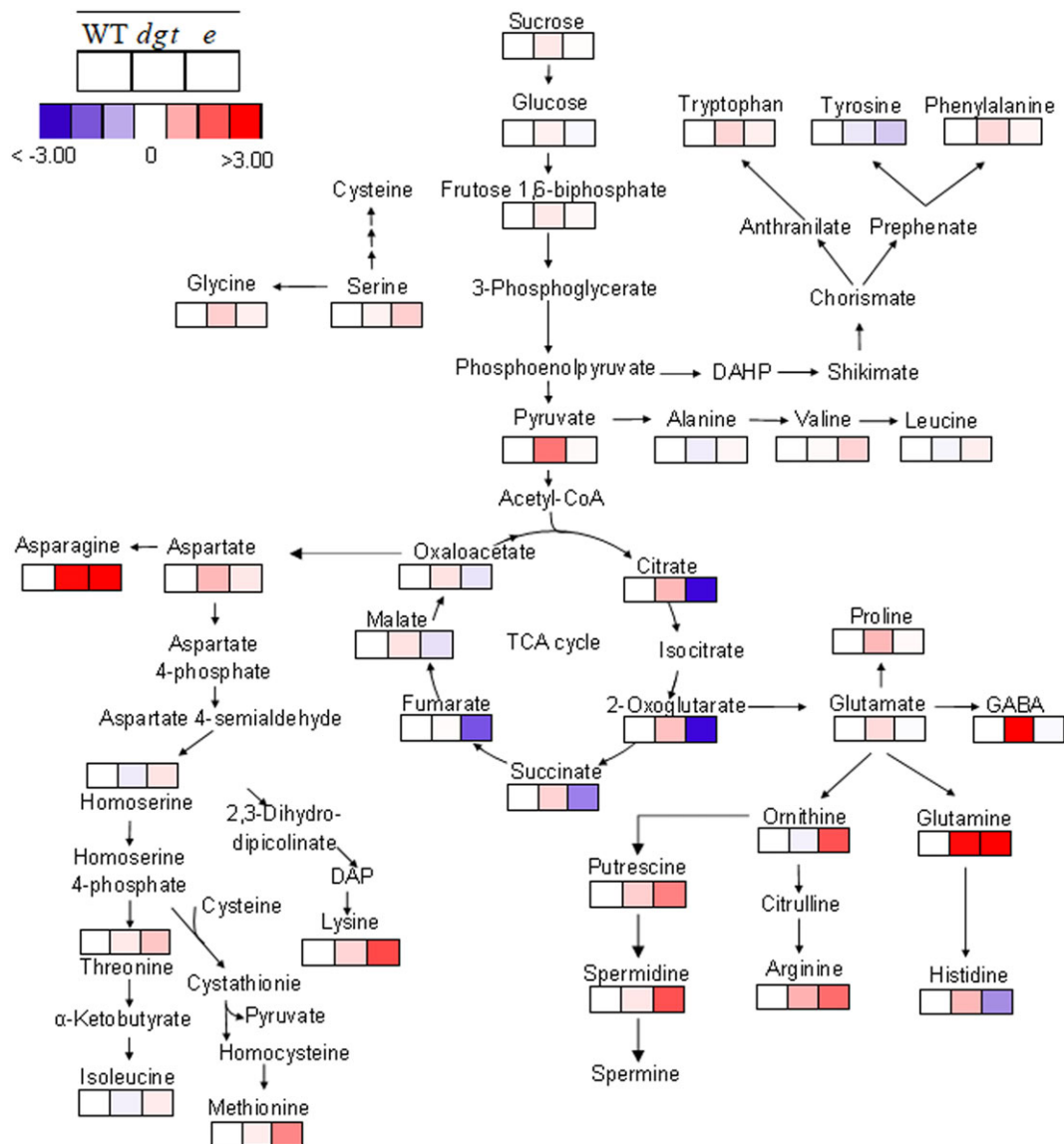


**FIGURE 5** Auxin signalling affects the relative metabolite content in tomato leaves. Changes in the relative metabolite content of tomato plants with either increased (*entire*) or reduced (*diageotropica*, *dgt*) auxin signalling were compared to wild-type (WT) plants growing under optimal conditions. Amino acids, organic acids, sugars, and sugar alcohols were determined by GC-MS as described in Section 2. The full data sets from these metabolic profiling studies are additionally available in Table S3. Data are normalized with respect to the average response calculated for the corresponding WT (to allow statistical assessment, individual plants from this set were normalized in the same way). Different colors represent levels of metabolite fold change where red is increasing and blue is decreasing. Data were normalized with respect to mean response calculated from wild type. Values are presented as means  $\pm$  SE ( $n = 6$ )

*entire* plants when compared with WT and *dgt* (Figure 5 and Table S5). Notably, ascorbate and dehydroascorbate were increased only in the *dgt* mutant. A similar trend is also observed for sugar content in which *dgt* plants display significantly increases in ribulose, glucose, fructose, and sucrose, whereas maltose, ribose, and ribulose were reduced in *entire* plants (Table S5). On assaying the levels of pyridine dinucleotides and their ratios, we observed only few changes in the pyridine nucleotides either at oxidized ( $\text{NAD}^+$  and  $\text{NADP}^+$ ) or at reduced ( $\text{NADH}$  and  $\text{NADPH}$ ) without changes in the ratio  $\text{NADH}/\text{NADP}^+$  and  $\text{NADPH}/\text{NADP}^+$  (Table S6). Remarkably, higher levels of  $\text{NAD}^+$  and  $\text{NADH}$  were observed in the *dgt* mutant when compared with WT and *entire*, whereas decreased levels of  $\text{NAD}^+$  and  $\text{NADP}^+$  were observed only in *entire*.

### 3.5 | Increased auxin signalling in *entire* affects the flux through the TCA cycle

Given the changes in  $R_d$ , sugar, and organic acid contents described above, we next decided to assess the rate of respiration under normal growth conditions by performing two complementary approaches. We directly evaluated the rate of  $R_L$  in the mutant lines (*dgt* and *entire*) by measuring the  $^{14}\text{CO}_2$  evolution following incubation of leaf discs with positionally labelled  $^{14}\text{C}$ -glucose ( $^{14}\text{C}$ -Glc) to assess the relative rate of flux through the TCA cycle and the metabolic flux analysis using  $^{14}\text{C}$ -label (Figure 6 and Table 4). This information is of pivotal significance given that metabolic pathways, and the key regulatory points thereof can be deduced using isotopically labelled substrates (Batista Silva,

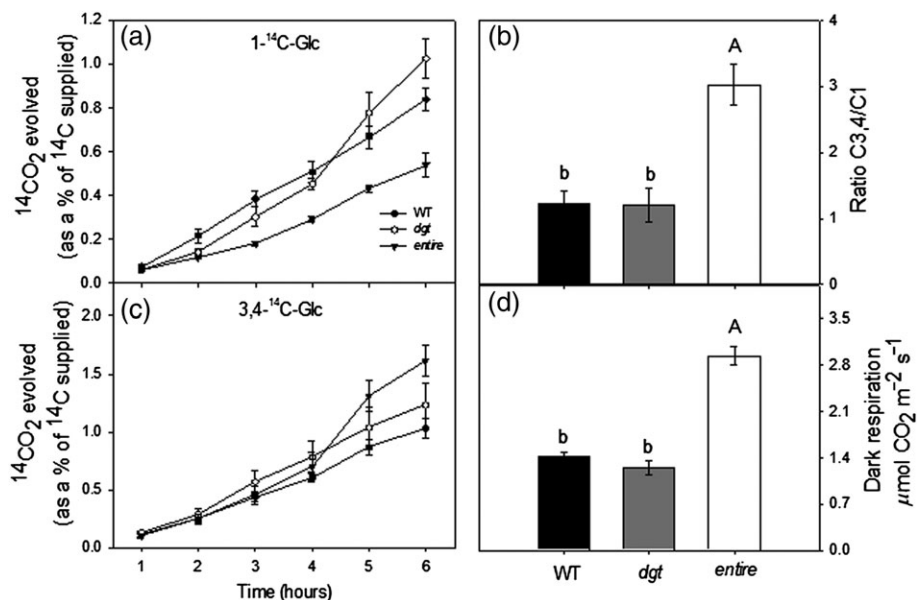


**FIGURE 6** Respiratory parameters are affected in leaf samples of auxin signalling mutants. Changes in respiration of tomato plants with either increased (*entire*) or reduced (*diageotropica*, *dgt*) auxin signalling were compared with wild-type (WT) plants growing under optimal conditions. Evolution of  $^{14}\text{CO}_2$  from isolated leaf discs in the light. The leaf discs were taken from 4-week-old plants and were incubated in 10-mM MES-KOH solution, pH 6.5, 0.3-mM glucose supplemented with 0.62 kBq ml $^{-1}$  of (a) [ $1\text{-}^{14}\text{C}$ ]-Glc or (b) [ $3,4\text{-}^{14}\text{C}$ ] at an irradiance of 100  $\mu\text{mol m}^{-2} \text{s}^{-1}$ . The  $\text{CO}_2$  liberated was captured at hourly intervals in a KOH trap and the amount of radiolabel released was subsequently quantified by liquid scintillation counting. (c) Ratio of carbon dioxide evolution from C3,4 to C1 position. (d) Dark respiration measurements performed in 4-week-old plants. WT, black bars; *dgt*, grey bars, *entire*, white bars. Values are presented as means  $\pm$  SE ( $n = 4$ ). Different letters represent average values that were judged to be statistically different between genotypes ( $P < 0.05$ , Tukey test)

Daloso, Fernie, Nunes-Nesi, & Araújo, 2016). For this purpose, we recorded the evolution of  $^{14}\text{CO}_2$  following incubation of leaf discs in light (approximately 150  $\mu\text{mol m}^{-2} \text{s}^{-1}$ ), supplied with [ $1\text{-}^{14}\text{C}$ ]-Glc and [ $3,4\text{-}^{14}\text{C}$ ]-Glc over a period of 6 hr. During this time, we collected the  $^{14}\text{CO}_2$  evolved at hourly intervals.  $\text{CO}_2$  can be released from the C1 position by the action of enzymes that are not associated with mitochondrial respiration; however, this does not happen for  $\text{CO}_2$  released from the C3/C4 position (Nunes-Nesi et al., 2007). Thus, the ratio of  $\text{CO}_2$  evolution from C3,4 to C1 position of Glc provides a strong indication of the TCA cycle regarding other carbohydrate oxidation process. When the relative  $^{14}\text{CO}_2$  release of the mutants and WT is compared for the various fed substrates, an interesting pattern emerges with a significant reduction occurring in the *entire* mutant following 3 hr of incubation with [ $1\text{-}^{14}\text{C}$ ]-Glc (Figure 6a). Thus, when supplied with [ $3,4\text{-}^{14}\text{C}$ ]-Glc, the  $^{14}\text{CO}_2$  release was significantly increased in the *entire* mutant from 5 hr onward (Figure 6b). Similarly, the C3,4/C1 ratio was significantly higher in the *entire* mutant in comparison with WT and *dgt* (Figure 6c), revealing that there is a higher proportion of carbohydrate oxidation by TCA cycle in illuminated leaves of *entire* plants. Our results are in close agreement with the results of our metabolic profiling as showed above. In the same vein,  $R_d$  measurements revealed an approximately 90% higher rates of  $\text{CO}_2$  evolution in *entire* plants when compared with both WT and *dgt* genotypes (Figure 6d).

We next assessed the redistribution of radiolabel by incubating excised leaf discs from 4-week-old plants of *dgt*, *entire*, and WT in [ $\text{U-}^{14}\text{C-Glu}$ ] for period of 3 hr. The genotypes were characterized by relatively similar total uptake; however, a differential radiolabel distribution was observed between genotypes (Table 4). Interestingly, when compared with WT and *entire* plants, the *dgt* mutant exhibited

higher values of incorporation in organic acid, sugars phosphate, soluble sugars, starch, total protein, and cell wall (Table 4). Thus, our data reveal a lower relative proportion of carbohydrate oxidation is performed by the TCA cycle in the plants with reduced sensitivity to auxin (*dgt* plants). In agreement with our metabolite profiles described above, the mutant *entire* was characterized by a significant increased radiolabel distribution to organic acids with reduced soluble sugars without changes in starch (Table 4). These results are in close agreement with the observation of changes of  $R_d$  in these plants. By contrast, *entire* mutant plants displayed an accelerated rate of oxidation of carbohydrates coupled with increases in respiratory rate under light conditions as well as increased dark respiration (Figure 6d and Table 4).

## 4 | DISCUSSION

### 4.1 | Photosynthetic capacity and metabolism adjustments in response to the modulation in auxin signalling

Auxin acts as a general coordinator of plant growth and development mainly by relaying information over both long and short ranges (Leyser, 2017). The major mechanism by which auxin affects cellular responses is via changes in transcription, and thus, several genes change their expression profile rapidly in response to auxin (Paponov et al., 2008). In addition, auxin is able to promote cell division in cultured cellular suspensions, which is accompanied by increased respiration (Leonova et al., 1985). It has been suggested that stimulation of

**TABLE 4** Respiratory carbon distribution is affected in leaf samples of auxin signalling mutants

Parameter*	WT	dgt	entire
Label incorporated (Bq g <sup>-1</sup> FW)			
Total uptake	111.52 ± 16.48 a	153.71 ± 24.34 a	117.02 ± 5.43 a
OA + Hexose-P	22.97 ± 4.57 b	49.90 ± 7.56 a	35.99 ± 1.50 ab
Amino acids	3.13 ± 0.42 b	6.42 ± 0.56 a	4.66 ± 0.68 ab
Soluble sugars	61.61 ± 13.04 b	94.74 ± 10.24 a	47.62 ± 3.09 c
Starch	14.43 ± 2.31 b	26.71 ± 4.01 a	17.03 ± 1.22 ab
Protein	0.66 ± 0.02 c	1.19 ± 0.17 a	0.92 ± 0.09 b
Cell wall	8.70 ± 0.25 c	16.50 ± 2.83 a	10.77 ± 0.50 b
Starch/Sucrose	0.24 ± 0.03 b	0.27 ± 0.26 ab	0.35 ± 0.015 a
Redistribution of radiolabel (as percentage of total assimilated)			
OA + Hexose-P	21.19 ± 4.37 b	26.65 ± 1.08 ab	34.73 ± 1.27 a
Amino acids	2.99 ± 0.35 a	3.53 ± 0.51 a	3.56 ± 0.18 a
Soluble sugars	55.40 ± 4.73 a	46.21 ± 0.79 b	39.66 ± 0.66 c
Starch	13.05 ± 0.46 a	14.20 ± 0.53 a	13.32 ± 0.65 a
Protein	0.63 ± 0.06 a	0.67 ± 0.09 a	0.74 ± 0.11 a
Cell wall	6.81 ± 0.96 a	8.66 ± 0.21 a	7.97 ± 0.29 a

Note. Changes in respiratory carbon redistribution of radiolabel carbon after incubation in [<sup>14</sup>C]-glucose of tomato plants with either increased (*entire*) or reduced (*diageotropica*, *dgt*) auxin signalling and were compared with wild-type (WT) plants growing under optimal conditions. Values are presented as means ± SE (n = 4). Different letters represent average values that were judged to be statistically different between genotypes (P < 0.05, Tukey test).

\*Leaf discs were cut from six separate plants of each genotype at the end of the night and illuminated at 150-μmol photons m<sup>-2</sup> s<sup>-1</sup> of PAR in Erlenmeyer flasks containing 0.62 kBq ml<sup>-1</sup> of unlabelled [U-<sup>14</sup>C-Glu]. After 3 hr, the leaf discs were extracted and fractionated. FW, fresh weight and OA, Organic Acids.

cell expansion is usually accompanied by the promotion of respiration (Bonner & Bandurski, 1952). Indeed, auxin can modulate plant growth by impacting innumerable processes such as photosynthesis and respiration (Bhardwaj et al., 2015; Ivanova et al., 2014). However, the link between auxin signalling and carbon metabolism in autotrophic tissues remains poorly understood. Combining physiological and biochemical approaches, we provide further evidence that auxin signalling plays an important role in growth modulation associated with carbon metabolism although the precise mechanistic link remains to be identified. Two contrasting mutants exhibiting either reduced (*dgt*) or increased (*entire*) auxin signalling were used to provide evidence for a crucial role of this hormone on the regulation of photosynthesis and indeed primary metabolism in general within the illuminated leaf. We demonstrated that several anatomical parameters were strongly affected, culminating in significant changes in photosynthetic and respiratory capacity (Table 1 and Figure S5–S6). Our results provide evidence that alterations in auxin signalling tightly controls plant morphology in agreement with Silva et al. (2018), culminating in altered photosynthesis and linking with TCA cycle activity (Tables 2 and 3). Reduced auxin signalling observed in *dgt* plants decreases the stomatal pore area but increases stomatal density in both sides of the leaf surface, resulting in higher water-use efficiency (Table 1 and Figure S5). In fact, auxin regulates stomatal patterning and development, basically by changes in its levels during stomatal development (Le, Liu, et al., 2014; Le, Zou, Yang, & Wang, 2014). Stomatal apertures are the major

gateway for the movement of CO<sub>2</sub> from the atmosphere into the mesophyll of leaves, controlling the movement of gases that also results in water vapour loss. Accordingly, *dgt* showed reduced water loss (Figure S3), which can also be explained by increases in the size of the leaf blade and reductions in total leaf area (Table 1 and Figure S5). Interestingly, even with increased SLA and thickness of the leaf blade, changes in *g<sub>m</sub>* in comparison with WT were not observed in *dgt* plants.

Our results also revealed that increased auxin signalling in *entire* plants is associated with enhanced photosynthetic capacity under ambient CO<sub>2</sub> concentration as well as elevated transpiratory rates (*E*), which are most likely a consequence of higher stomatal conductance (*g<sub>s</sub>*) and increased *V<sub>cmax</sub>* and *J<sub>max</sub>* on a *C<sub>c</sub>* basis. Although these results correlate with improved plant biomass under optimal growth conditions, it should be kept in mind that under low water availability, the lower *WUE<sub>i</sub>* presented by *entire* plants represents a highly undesirable trait (Xu & Zhou, 2008). Considering the importance of auxin in leaf venation patterning and xylem development in angiosperms, as well as stomatal cell morphology, this hormone may play an instrumental role in the ecological success of angiosperms plants (Zhao, 2010). The link between auxin biosynthesis and maximum photosynthetic rate through leaf venation has been recently demonstrated, providing strong support to the theory that an increase in leaf vein density, coupled with their efficient placement, can drive increases in leaf photosynthetic capacity (McAdam et al., 2017). Identification of the precise mechanism regulating this key anatomical feature and the exact nature of auxin in the regulation of photosynthetic capacity remain important open questions that should be further addressed.

## 4.2 | Respiratory metabolism is affected by changes in auxin signalling

Our results further demonstrate that enhanced auxin signalling observed in *entire* leads to increase not only in growth (Figure 1) but also in respiratory and photosynthetic rates (Table 2). By using complementary approaches, we further confirmed that *entire* plants had increased respiration rates both in the dark and during the day (Figure 6), providing evidence that increased auxin signalling present in *entire* plants stimulates respiration. In agreement with this observation, it has been suggested that auxin may increase respiration rate indirectly through increased supply of adenosine diphosphate (ADP) by promoting a rapid utilization of ATP in the expanding cells (French & Beevers, 1953). We further observed that *dgt* plants seem to use less transitory starch during the night leading to significant accumulation of different respiratory substrates (e.g., sugars and organic acids), resulting in lower growth during the vegetative stage (Figures 4 and 5). As previously demonstrated, starch is typically degraded in a near-linear manner, with around 5–10% remaining at the end of the night producing sucrose readily available for sustaining growth (Gibon et al., 2004; Gibon et al., 2009; Smith & Stitt, 2007). Usually, plants that accumulate more starch during the day degrade it faster at night, and as a result, a small amount of starch still remains at the end of the night (Gibon et al., 2004; Gibon et al., 2009). Therefore, the transient imbalance between the supply and utilization of C is directly connected with plant growth performance, and this can be illustrated in



mutants that are defective in the synthesis or degradation of starch. As observed in *dgt* plants, in starchless mutants defective in Phosphoglucomutase (*pgm*), sugar accumulation is observed with a concomitant growth inhibition (Caspar, Huber, & Somerville, 1985; Smith & Stitt, 2007; Stitt, Gibon, Lunn, & Piques, 2007). Additionally, the adjustment of starch turnover to a decreased C supply must be accompanied by a compensatory decrease in the rate of C utilization for respiratory and growth process (Smith & Stitt, 2007; Stitt et al., 2007; Stitt & Zeeman, 2012). The relationship between high respiratory rate and rapid growth could be explained, at least partially, by the importance of the TCA cycle activity in the regulation of the photosynthesis in illuminated leaves, once the balance between C supply and demand optimize the capacity to growth (Nunes-Nesi, Araújo, & Fernie, 2011; Smith & Stitt, 2007). Nevertheless, the metabolic and molecular cues underlying such connections remain contentious, and therefore, further work is still required to establish how exactly auxin signalling is able to impact both photosynthesis and respiration.

A growing body of evidence shows that premature or incomplete exhaustion of starch results in lower growth rates and that this balance requires appropriate changes in the rates of starch synthesis and degradation (Smith & Stitt, 2007; Stitt & Zeeman, 2012). Even small disturbances in leaf starch turnover affect metabolism and growth. As such, incomplete exhaustion of starch during the night (Figure 4) leading to an inefficient usage of carbon pool, coupled with reduced respiration rates (Table 2) in *dgt* plants, might explain, at least partially, the reduced growth observed (Figure 2). Considering that starch is a major integrator in the regulation of plant growth to cope with fluctuations in the C and energy status of the plant (Sulpice et al., 2009), it is not surprising that starch biosynthesis in leaves is highly regulated at multiple levels in response to distinct signals including sugars and hormones such as cytokinins (Bahaji et al., 2015), abscisic acid (Ramon, Rolland, Thevelein, Van Dijck, & Leyman, 2007), brassinosteroids (Oh et al., 2011), and more recently, also auxin (Mishra, Singh, Aggrawal, & Laxmi, 2009; Sagar et al., 2013). Moreover, auxin acts as a repressor of starch accumulation directly by negatively controlling the expression of ADP-glucose pyrophosphorylase in an antagonistic manner to cytokinin (Miyazawa et al., 1999). In the same vein, Sagar et al. (2013) have shown that AUXIN RESPONSIVE FACTOR 4 (ARF4) is involved in the control of the sugar content of tomato fruits, mainly by upregulation of genes and enzyme activities involved in starch biosynthesis, especially genes coding for ADP-glucose pyrophosphorylase. In rice, an auxin response factor, OSARF18, plays a positive role of auxin signalling in starch synthesis (Huang, Li, & Zhao, 2016). Moreover, in tobacco cells treated with exogenous auxin, downregulation of starch-related genes was observed (Miyazawa et al., 1999). In root tips of *Arabidopsis*, starch granule production is inhibited by the constitutive expression of an auxin action repressor from rice (Luo et al., 2015).

These findings indicate that auxin most likely impacts starch accumulation upstream of starch biosynthesis and degradation. The precise pattern of consumption of starch during the night in *entire* plants (Figure 4) coupled with enhanced respiration rates (Table 2) might also explain why higher biomass was observed in this genotype. It should also be mentioned that the profile of both organic acids and amino acids as well as polyamines was strongly affected in *entire* plants.

The majority of organic acids including citrate, isocitrate, 2-oxoglutarate, succinate, and fumarate were decreased in *entire* plants, whereas branched-chain amino acids were reduced only in the *dgt* mutant, with few variations on TCA cycle intermediates, suggesting that *dgt* mutant is using branched-chain amino acids more efficiently as alternative respiratory substrates. Accordingly, carbon skeletons from amino acids can be converted to precursors or intermediates of the TCA cycle to support mitochondrial metabolism and ATP biosynthesis, whereas oxidation of certain amino acids (e.g., leucine, isoleucine, valine, lysine, and proline) can directly provide electrons into the mitochondrial electron transport chain (Araújo et al., 2010; Hildebrandt, Nunes-Nesi, Araújo, & Braun, 2015). As such, the elevated  $R_d$  and  $R_L$  (Figure 6 and Table 2) coupled with changes in the evolution of radiolabeled  $CO_2$  observed in *entire* plants provide further support to our hypothesis that the TCA cycle is working faster in the auxin signalling enhanced *entire* mutant. In good agreement with our results obtained in terms of growth and metabolic adjustments in auxin signalling mutants, we also identified an interestingly accumulation of polyamines (PAs), mainly in *entire* mutant (Figure 5 and Table S5). Notably, PAs plays a pivotal role in the regulation of plant development, and it is involved in several physiological processes (Kusano, Yamaguchi, Berberich, & Takahashi, 2007). Together with glutamine and orthithine, PAs are part of the overall metabolism of nitrogenous compounds, and accordingly, putrescine, spermidine, and spermine are associated with nitrate nutrition, acting as a metabolic buffer and maintaining the cellular pH under conditions where ammonium assimilation occurs (Altman & Levin, 1993). In leaves, glutamate, glutamine, aspartate, and asparagine are primary products of nitrogen assimilation and therefore contributing to plant growth and biomass accumulation (Lam et al., 1995). Our results suggest therefore that increasing auxin signalling by changes in *IAA9* expression impacts nitrogen metabolism and increases plant growth partly explained by the action of PAs triggering plant growth and development (Marco, Alcázar, Tiburcio, & Carrasco, 2011). In contrast, *dgt* does not seem to be affected when compared with WT, which can, at least partially, be explained by the relatively few changes in TCA cycle intermediates or even in amino acids involved in nitrogen metabolism. Finally, changes in gene expression that only occur in the *entire* mutant could be potentially good candidates for explaining physiological and metabolic changes that occur only in this mutant, such as the consequences of auxin on PA and nitrogen metabolism.

### 4.3 | DGT modulates Aux/IAA and ARF families gene expression

Given the strong auxin-associated phenotypes of the mutants, we investigated the effect of downregulation of the *SIIAA9* (*entire*) and *DGT* on the expression of auxin responsive genes. The downregulation of *SIIAA9* resulted in alteration of several genes members of the same family such as *IAA2*, *IAA3*, *IAA19*, and *IAA29* as well as the *GH3* gene, which is related to auxin homeostasis. Accordingly, the mutation in *SIIAA9* seems to alter the expression pattern of other genes from the same family, once the endogenous levels of auxin are differentially perceived, selectively controlling the expression of *SIIAA3* (Wang et al., 2009). Moreover, this downregulation also increases the

expression of *SI1AA19* and *SI1AA29*, as well as *ARF2* and *ARF8*, which may contribute to the reduced auxin-responsiveness in *IAA3* mutant plants (Chaabouni et al., 2009). Our findings strongly support the hypothesis that different members of the Aux/IAA family are involved in distinct developmental processes, which can be considered as an important gene family to be further investigated in order to elucidate their agricultural importance.

The mutation in *DIAGEOTROPICA* appears to be able not only to modulate the expression of the genes of the Aux/IAA family, as shown before by Nebenführ, White, and Lomax (2000), but also to affect the expression of members of the ARFs family (*ARF8* and *ARF10*; Figure 2). Collectively, our results confirm that *dgt* participates in auxin signal transduction and suggest a specific controlling mechanism in ARF gene family. Additionally, our results also suggest that the lack of *dgt* function can also regulate *SIARF*s genes increasing the expression of *SIARF8* and *SIARF10*, which are both expressed in leaves. The ARF gene family specifically controls auxin-dependent biological responses (Zouine et al., 2014). Interestingly, both *SIARF8* and *SIARF10* are involved in similar processes during plant growth and development. The expression profile observed here suggests that the product of *DGT* seems to be not only an important player in leaf metabolism (Figure 5) but is also able to modulate important genes associated with fruit set and yield (Figure 2).

## 5 | CONCLUDING REMARKS

In summary, our study brings novel insights into the ability of auxin signalling genes to control plant growth by adjusting leaf development and central metabolism, simultaneously impacting both photosynthetic and respiratory metabolism. Taken together, our findings indicated that auxin signalling is a regulatory control point of not only developmental but also metabolic processes including mitochondrial and chloroplastidic metabolism in autotrophic tissues. Remarkably, changes in auxin signalling are likely to impact not only carbon assimilation and growth but also how plants rely on organic acids and amino acid metabolism to support respiratory processes coupled to changes in starch metabolism. Collectively, the results presented here demonstrated that changes in auxin signalling are of crucial significance in the regulation of both anatomical and physiological aspects that are seemingly important to mediate plant growth and function. Our observations also highlight the integration of primary metabolisms and plant development as a novel avenue in auxin signalling manipulation for agronomic purposes. However, further experimentation focusing at the level of guard cell development and function in response to changes in auxin signalling will be required to fully define the precise mechanism by which energy metabolism and hormone-mediated control of growth are associated, as well as the significance of this connection in response to suboptimal environmental conditions.

## ACKNOWLEDGMENTS

Discussions with Prof. Dimas M. Ribeiro, Prof. Fábio M. DaMatta, and Prof. Samuel C.V. Martins (all from Universidade Federal de Viçosa, Brazil) were highly valuable in the development of this work. This work was supported by funding from the Max Planck Society (to W.

L. A.), the Conselho Nacional de Desenvolvimento Científico e Tecnológico (CNPq-Brazil to W. L. A.), the Fundação de Amparo à Pesquisa do Estado de Minas Gerais (FAPEMIG-Brazil, Grants APQ-01078-15 and APQ-01357-14 to A. N. N. and W. L. A.), and the Foundation for Research Assistance of the São Paulo State (FAPESP-Brazil, grant 2014/16553-1). We also thank the scholarships granted by the Brazilian Federal Agency for Support and Evaluation of Graduate Education (CAPES-Brazil) to W. B. S. D. B. M. was supported by a CAPES post-doctoral grant. Research fellowships granted by CNPq-Brazil to A. N. N. and W. L. A. are also gratefully acknowledged.

## ORCID

Willian Batista-Silva  <http://orcid.org/0000-0003-1144-1656>

Adriano Nunes-Nesi  <http://orcid.org/0000-0002-9581-9355>

Wagner L. Araújo  <http://orcid.org/0000-0002-4796-2616>

## REFERENCES

- Altman, A., & Levin, N. (1993). Interactions of polyamines and nitrogen nutrition in plants. *Physiologia Plantarum*, *89*, 653–658.
- ap Rees, T., & Beevers, H. (1960). Pathways of glucose dissimilation in carrot slices. *Plant Physiology*, *35*, 830–838.
- Araújo, W. L., Ishizaki, K., Nunes-Nesi, A., Larson, T. R., Tohge, T., Krahnert, I., ... Graham, I. A. (2010). Identification of the 2-hydroxyglutarate and isovaleryl-CoA dehydrogenases as alternative electron donors linking lysine catabolism to the electron transport chain of Arabidopsis mitochondria. *The Plant Cell*, *22*, 1549–1563.
- Araújo, W. L., Nunes-Nesi, A., Nikoloski, Z., Sweetlove, L. J., & Fernie, A. R. (2012). Metabolic control and regulation of the tricarboxylic acid cycle in photosynthetic and heterotrophic plant tissues. *Plant, Cell & Environment*, *35*, 1–21.
- Araújo, W. L., Nunes-Nesi, A., Osorio, S., Usadel, B., Fuentes, D., Nagy, R., ... Tohge, T. (2011). Antisense inhibition of the iron-sulphur subunit of succinate dehydrogenase enhances photosynthesis and growth in tomato via an organic acid-mediated effect on stomatal aperture. *The Plant Cell*, *23*, 600–627.
- Audran-Delalande, C., Bassa, C., Mila, I., Regad, F., Zouine, M., & Bouzayen, M. (2012). Genome-wide identification, functional analysis and expression profiling of the Aux/IAA gene family in tomato. *Plant and Cell Physiology*, *53*, 659–672.
- Bahaji, A., Sánchez-López, Á. M., De Diego, N., Muñoz, F. J., Baroja-Fernández, E., Li, J., ... Almagro, G. (2015). Plastidic phosphoglucose isomerase is an important determinant of starch accumulation in mesophyll cells, growth, photosynthetic capacity, and biosynthesis of plastidic cytokinins in Arabidopsis. *PLoS One*, *10*, e0119641.
- Batista Silva, W., Daloso, D. M., Fernie, A. R., Nunes-Nesi, A., & Araújo, W. L. (2016). Can stable isotope mass spectrometry replace radiolabelled approaches in metabolic studies? *Plant Science*, *249*, 59–69.
- Berger, D., & Altmann, T. (2000). A subtilisin-like serine protease involved in the regulation of stomatal density and distribution in Arabidopsis thaliana. *Genes & Development*, *14*, 1119–1131.
- Berkowitz, O., De Clercq, I., Van Breusegem, F., & Whelan, J. (2016). Interaction between hormonal and mitochondrial signalling during growth, development and in plant defence responses. *Plant, Cell & Environment*, *39*, 1127–1139.
- Bhardwaj, R., Kaur, R., Bali, S., Kaur, P., Sirhindi, G., Thukral, A. K., ... Vig, A. P. (2015). Role of various hormones in photosynthetic responses of green plants under environmental stresses. *Current Protein and Peptide Science*, *16*, 435–449.
- Bonner, J., & Bandurski, R. S. (1952). Studies of the physiology, pharmacology, and biochemistry of the auxins. *Annual Review of Plant Physiology*, *3*, 59–86.

- Carvalho, R. F., Campos, M. L., Pino, L. E., Crestana, S. L., Zsögön, A., Lima, J. E., ... Peres, L. E. (2011). Convergence of developmental mutants into a single tomato model system: 'Micro-Tom' as an effective toolkit for plant development research. *Plant Methods*, 7, 18.
- Caspar, T., Huber, S. C., & Somerville, C. (1985). Alterations in growth, photosynthesis, and respiration in a starchless mutant of *Arabidopsis thaliana* (L.) deficient in chloroplast phosphoglucomutase activity. *Plant Physiology*, 79, 11–17.
- Chaabouni, S., Jones, B., Delalande, C., Wang, H., Li, Z., Mila, I., ... Bouzayen, M. (2009). SI-IAA3, a tomato Aux/IAA at the crossroads of auxin and ethylene signalling involved in differential growth. *Journal of Experimental Botany*, 60, 1349–1362.
- Christian, M., Steffens, B., Schenck, D., & Lüthen, H. (2003). The diageotropica mutation of tomato disrupts a signalling chain using extracellular auxin binding protein 1 as a receptor. *Planta*, 218, 309–314.
- Davis, P. (2005). *Plant hormones: Biosynthesis, signal transduction, action*. The Netherlands: Publisher Springer.
- Delker, C., Raschke, A., & Quint, M. (2008). Auxin dynamics: the dazzling complexity of a small molecule's message. *Planta*, 227(5), 929–941.
- Devoghalaere, F., Doucen, T., Guitton, B., Keeling, J., Payne, W., Ling, T. J., ... Dayatilake, G. (2012). A genomics approach to understanding the role of auxin in apple (*Malus x domestica*) fruit size control. *BMC Plant Biology*, 12, 7.
- Enders, T. A., & Strader, L. C. (2015). Auxin activity: Past, present, and future. *American Journal of Botany*, 102, 180–196.
- Ethier, G., & Livingston, N. (2004). On the need to incorporate sensitivity to CO<sub>2</sub> transfer conductance into the Farquhar–von Caemmerer–Berry leaf photosynthesis model. *Plant, Cell & Environment*, 27, 137–153.
- Farquhar, G.v., von Caemmerer, S.v., & Berry, J. (1980). A biochemical model of photosynthetic CO<sub>2</sub> assimilation in leaves of C<sub>3</sub> species. *Planta*, 149, 78–90.
- Feder, N., & O'Brien, T. (1968). Plant microtechnique: Some principles and new methods. *American Journal of Botany*, 55, 123–142.
- Fernie, A. R., Aharoni, A., Willmitzer, L., Stitt, M., Tohge, T., Kopka, J., ... DeLuca, V. (2011). Recommendations for reporting metabolite data. *The Plant Cell*, 23, 2477–2482.
- Fernie, A. R., Roscher, A., Ratcliffe, R. G., & Kruger, N. J. (2001). Fructose 2, 6-bisphosphate activates pyrophosphate: fructose-6-phosphate 1-phosphotransferase and increases triose phosphate to hexose phosphate cycling in heterotrophic cells. *Planta*, 212, 250–263.
- Fernie, A. R., Trethewey, R. N., Krotzky, A. J., & Willmitzer, L. (2004). Metabolite profiling: from diagnostics to systems biology. *Nature Reviews Molecular Cell Biology*, 5, 763–769.
- French, R. C., & Beevers, H. (1953). Respiratory and growth responses induced by growth regulators and allied compounds. *American Journal of Botany*, 40, 660–666.
- Gao, J., Cao, X., Shi, S., Ma, Y., Wang, K., Liu, S., ... Ma, H. (2016). Genome-wide survey of Aux/IAA gene family members in potato (*Solanum tuberosum*): Identification, expression analysis, and evaluation of their roles in tuber development. *Biochemical and Biophysical Research Communications*, 471, 320–327.
- Genty, B., Briantais, J.-M., & Baker, N. R. (1989). The relationship between the quantum yield of photosynthetic electron transport and quenching of chlorophyll fluorescence. *Biochimica et Biophysica Acta (BBA) - General Subjects*, 990, 87–92.
- Gibon, Y., Bläsing, O. E., Palacios-Rojas, N., Pankovic, D., Hendriks, J. H., Fisahn, J., ... Stitt, M. (2004). Adjustment of diurnal starch turnover to short days: Depletion of sugar during the night leads to a temporary inhibition of carbohydrate utilization, accumulation of sugars and post-translational activation of ADP-glucose pyrophosphorylase in the following light period. *The Plant Journal*, 39, 847–862.
- Gibon, Y., Pyl, E. T., Sulpice, R., Lunn, J. E., Hoehne, M., Guenther, M., & Stitt, M. (2009). Adjustment of growth, starch turnover, protein content and central metabolism to a decrease of the carbon supply when *Arabidopsis* is grown in very short photoperiods. *Plant, Cell & Environment*, 32, 859–874.
- Gilbert, M. E., Pou, A., Zwieniecki, M. A., & Holbrook, N. M. (2012). On measuring the response of mesophyll conductance to carbon dioxide with the variable J method. *Journal of Experimental Botany*, 63, 413–425.
- Grassi, G., & Magnani, F. (2005). Stomatal, mesophyll conductance and biochemical limitations to photosynthesis as affected by drought and leaf ontogeny in ash and oak trees. *Plant, Cell & Environment*, 28, 834–849.
- Harley, P. C., Loreto, F., Di Marco, G., & Sharkey, T. D. (1992). Theoretical considerations when estimating the mesophyll conductance to CO<sub>2</sub> flux by analysis of the response of photosynthesis to CO<sub>2</sub>. *Plant Physiology*, 98, 1429–1436.
- Hedden, P., & Thomas, S. G. (2008). *Annual plant reviews, plant hormone signaling* (Vol. 24). John Wiley & Sons.
- Hermida-Carrera, C., Kapralov, M. V., & Galmés, J. (2016). Rubisco catalytic properties and temperature response in crops. *Plant Physiology*, 171, 2549–2561.
- Hildebrandt, T. M., Nunes-Nesi, A., Araújo, W. L., & Braun, H.-P. (2015). Amino acid catabolism in plants. *Molecular Plant*, 8, 1563–1579.
- Huang, G., Li, T., Li, X., Tan, D., Jiang, Z., Wei, Y., ... Wang, A. (2014). Comparative transcriptome analysis of climacteric fruit of Chinese pear (*Pyrus ussuriensis*) reveals new insights into fruit ripening. *PLoS One*, 9, e107562.
- Huang, J., Li, Z., & Zhao, D. (2016). Deregulation of the OsmiR160 target gene OsARF18 causes growth and developmental defects with an alteration of auxin signaling in rice. *Scientific Reports*, 6, 29938.
- Hunt, R., Causton, D., Shipley, B., & Askew, A. (2002). A modern tool for classical plant growth analysis. *Annals of Botany*, 90, 485–488.
- Ivanchenko, M. G., Zhu, J., Wang, B., Medvecká, E., Du, Y., Azzarello, E., ... Dubrovsky, J. G. (2015). The cyclophilin A DIAGEOTROPICA gene affects auxin transport in both root and shoot to control lateral root formation. *Development*, 142, 712–721.
- Ivanova, A., Law, S. R., Narsai, R., Duncan, O., Lee, J.-H., Zhang, B., ... Radomiljac J.D.; van der Merwe M. & Yi K. (2014). A functional antagonistic relationship between auxin and mitochondrial retrograde signaling regulates alternative oxidase1a expression in *Arabidopsis*. *Plant Physiology*, 165, 1233–1254.
- Jing, H., Yang, X., Zhang, J., Liu, X., Zheng, H., Dong, G., ... Qian, Q. (2015). Peptidyl-prolyl isomerization targets rice Aux/IAAs for proteasomal degradation during auxin signalling. *Nature Communications*, 6.
- Kelly, M. O., & Bradford, K. J. (1986). Insensitivity of the diageotropica tomato mutant to auxin. *Plant Physiology*, 82, 713–717.
- Kopka, J., Schauer, N., Krueger, S., Birkemeyer, C., Usadel, B., Bergmüller, E., ... Stitt, M. (2004). GMD@ CSB. . DB: The Golm Metabolome Database. *Bioinformatics*, 21, 1635–1638.
- Kusano, T., Yamaguchi, K., Berberich, T., & Takahashi, Y. (2007). Advances in polyamine research in 2007. *Journal of Plant Research*, 120, 345–350.
- Lam, H.-M., Coschigano, K., Schultz, C., Melo-Oliveira, R., Tjaden, G., Oliveira, I., ... Coruzzi, G. (1995). Use of *Arabidopsis* mutants and genes to study amide amino acid biosynthesis. *The Plant Cell*, 7, 887–898.
- Laskowski, M., Grieneisen, V. A., Hofhuis, H., Colette, A., Hogeweg, P., Marée, A. F., & Scheres, B. (2008). Root system architecture from coupling cell shape to auxin transport. *PLoS Biology*, 6, e307.
- Lavy, M., Prigge, M. J., Tigyi, K., & Estelle, M. (2012). The cyclophilin DIAGEOTROPICA has a conserved role in auxin signaling. *Development*, 139, 1115–1124.
- Le, J., Liu, X.-G., Yang, K.-Z., Chen, X.-L., Zou, J.-J., Wang, H.-Z., ... Sack, F. (2014). Auxin transport and activity regulate stomatal patterning and development. *Nature Communications*, 5.
- Le, J., Zou, J., Yang, K., & Wang, M. (2014). Signaling to stomatal initiation and cell division. Regulation of Cell Fate Determination in Plants, 56.



- Leonova, L., Gamborg, K., Vojnikov, V., & Varakina, N. (1985). Promotion of respiration by auxin in the induction of cell division in suspension culture. *Journal of Plant Growth Regulation*, 4, 169–176.
- Leyser, O. (2017). Auxin Signaling. *Plant Physiology*. <https://doi.org/10.1104/pp.17.00765>
- Li, J., Khan, Z. U., Tao, X., Mao, L., Luo, Z., & Ying, T. (2017). Effects of exogenous auxin on pigments and primary metabolite profile of post-harvest tomato fruit during ripening. *Scientia Horticulturae*, 219, 90–97.
- Lisec, J., Schauer, N., Kopka, J., Willmitzer, L., & Fernie, A. R. (2006). Gas chromatography mass spectrometry-based metabolite profiling in plants. *Nature Protocols*, 1, 387–396.
- Logan, B. A., Adams, W. W., & Demmig-Adams, B. (2007). Viewpoint: Avoiding common pitfalls of chlorophyll fluorescence analysis under field conditions. *Functional Plant Biology*, 34, 853–859.
- Long, S., & Bernacchi, C. (2003). Gas exchange measurements, what can they tell us about the underlying limitations to photosynthesis? Procedures and sources of error. *Journal of Experimental Botany*, 54, 2393–2401.
- Luedemann, A., von Malotky, L., Erban, A., & Kopka, J. (2011). TagFinder: Preprocessing software for the fingerprinting and the profiling of gas chromatography-mass spectrometry based metabolome analyses. In *Plant Metabolomics* (pp. 255–286). Springer.
- Luo, S., Li, Q., Liu, S., Pinas, N. M., Tian, H., & Wang, S. (2015). Constitutive expression of OsIAA9 affects starch granules accumulation and root gravitropic response in Arabidopsis. *Frontiers in Plant Science*, 6, 1156.
- Lytovchenko, A., Sweetlove, L., Pauly, M., & Fernie, A. R. (2002). The influence of cytosolic phosphoglucomutase on photosynthetic carbohydrate metabolism. *Planta*, 215, 1013–1021.
- Marco, F., Alcázar, R., Tiburcio, A. F., & Carrasco, P. (2011). Interactions between polyamines and abiotic stress pathway responses unraveled by transcriptome analysis of polyamine overproducers. *OMICS*, 15, 775–781.
- McAdam, S. A., Eléouët, M. P., Best, M., Brodribb, T. J., Murphy, M. C., Cook, S. D., ... Gill, W. M. (2017). Linking auxin with photosynthetic rate via leaf venation. *Plant Physiology*, 175, 351–360.
- Medeiros, D. B., Martins, S. C., Cavalcanti, J. H. F., Daloso, D. M., Martinoia, E., Nunes-Nesi, A., ... Araújo, W. L. (2016). Enhanced photosynthesis and growth in atqac1 knockout mutants are due to altered organic acid accumulation and an increase in both stomatal and mesophyll conductance. *Plant Physiology*, 170, 86–101.
- Millar, A. H., Whelan, J., Soole, K. L., & Day, D. A. (2011). Organization and regulation of mitochondrial respiration in plants. *Annual Review of Plant Biology*, 62, 79–104.
- Mishra, B. S., Singh, M., Aggrawal, P., & Laxmi, A. (2009). Glucose and auxin signaling interaction in controlling Arabidopsis thaliana seedlings root growth and development. *PLoS One*, 4, e4502.
- Miyazawa, Y., Sakai, A., Miyagishima, S.-Y., Takano, H., Kawano, S., & Kuroiwa, T. (1999). Auxin and cytokinin have opposite effects on amyloplast development and the expression of starch synthesis genes in cultured bright yellow-2 tobacco cells. *Plant Physiology*, 121, 461–470.
- Muday, G. K., Lomax, T. L., & Rayle, D. L. (1995). Characterization of the growth and auxin physiology of roots of the tomato mutant, diageotropica. *Planta*, 195, 548–553.
- Murashige, T., & Skoog, F. (1962). A revised medium for rapid growth and bio assays with tobacco tissue cultures. *Physiologia Plantarum*, 15, 473–497.
- Nebenführ, A., White, T., & Lomax, T. L. (2000). The diageotropica mutation alters auxin induction of a subset of the Aux/IAA gene family in tomato. *Plant Molecular Biology*, 44, 73–84.
- Niinemets, Ü., Díaz-Espejo, A., Flexas, J., Galmés, J., & Warren, C. R. (2009). Role of mesophyll diffusion conductance in constraining potential photosynthetic productivity in the field. *Journal of Experimental Botany*, 60, 2249–2270.
- Nunes-Nesi, A., Araújo, W. L., & Fernie, A. R. (2011). Targeting mitochondrial metabolism and machinery as a means to enhance photosynthesis. *Plant Physiology*, 155, 101–107.
- Nunes-Nesi, A., Carrari, F., Gibon, Y., Sulpice, R., Lytovchenko, A., Fisahn, J., ... Fernie, A. R. (2007). Deficiency of mitochondrial fumarase activity in tomato plants impairs photosynthesis via an effect on stomatal function. *The Plant Journal*, 50, 1093–1106.
- Nunes-Nesi, A., Carrari, F., Lytovchenko, A., Smith, A. M., Loureiro, M. E., Ratcliffe, R. G., ... Fernie, A. R. (2005). Enhanced photosynthetic performance and growth as a consequence of decreasing mitochondrial malate dehydrogenase activity in transgenic tomato plants. *Plant Physiology*, 137, 611–622.
- Oh, K., Ivanchenko, M. G., White, T., & Lomax, T. L. (2006). The diageotropica gene of tomato encodes a cyclophilin: A novel player in auxin signaling. *Planta*, 224, 133–144.
- Oh, M.-H., Sun, J., Oh, D. H., Zielinski, R. E., Clouse, S. D., & Huber, S. C. (2011). Enhancing Arabidopsis leaf growth by engineering the BRASSINOSTEROID INSENSITIVE1 receptor kinase. *Plant Physiology*, 157, 120–131.
- Paponov, I. A., Paponov, M., Teale, W., Menges, M., Chakrabortee, S., Murray, J. A., & Palme, K. (2008). Comprehensive transcriptome analysis of auxin responses in Arabidopsis. *Molecular Plant*, 1, 321–337.
- Plaxton, W. C., & Tran, H. T. (2011). Metabolic adaptations of phosphate-starved plants. *Plant Physiology*, 156, 1006–1015.
- Pons, T. L., Flexas, J., Von Caemmerer, S., Evans, J. R., Genty, B., Ribas-Carbo, M., & Brugnoli, E. (2009). Estimating mesophyll conductance to CO<sub>2</sub>: Methodology, potential errors, and recommendations. *Journal of Experimental Botany*, 60(8), erp081.
- Porra, R., Thompson, W., & Kriedemann, P. (1989). Determination of accurate extinction coefficients and simultaneous equations for assaying chlorophylls a and b extracted with four different solvents: Verification of the concentration of chlorophyll standards by atomic absorption spectroscopy. *Biochimica et Biophysica Acta (BBA)-Bioenergetics*, 975, 384–394.
- Quint, M., & Gray, W. M. (2006). Auxin signaling. *Current Opinion in Plant Biology*, 9, 448–453.
- Ramon, M., Rolland, F., Thevelein, J. M., Van Dijck, P., & Leyman, B. (2007). ABI4 mediates the effects of exogenous trehalose on Arabidopsis growth and starch breakdown. *Plant Molecular Biology*, 63, 195–206.
- Rice, M. S., & Lomax, T. L. (2000). The auxin-resistant diageotropica mutant of tomato responds to gravity via an auxin-mediated pathway. *Planta*, 210, 906–913.
- Rodeghiero, M., Niinemets, Ü., & Cescatti, A. (2007). Major diffusion leaks of clamp-on leaf cuvettes still unaccounted: How erroneous are the estimates of Farquhar et al. model parameters? *Plant, Cell & Environment*, 30, 1006–1022.
- Roessner, U., Luedemann, A., Brust, D., Fiehn, O., Linke, T., Willmitzer, L., & Fernie, A. R. (2001). Metabolic profiling allows comprehensive phenotyping of genetically or environmentally modified plant systems. *The Plant Cell*, 13, 11–29.
- Sagar, M., Chervin, C., Mila, I., Hao, Y., Roustan, J.-P., Benichou, M., ... Latché, A. (2013). SIARF4, an auxin response factor involved in the control of sugar metabolism during tomato fruit development. *Plant Physiology*, 161, 1362–1374.
- Schneider, C. A., Rasband, W. S., & Eliceiri, K. W. (2012). NIH Image to ImageJ: 25 years of image analysis. *Nature Methods*, 9, 671–675.
- Sharkey, T. D., Bernacchi, C. J., Farquhar, G. D., & Singsaas, E. L. (2007). Fitting photosynthetic carbon dioxide response curves for C3 leaves. *Plant, Cell & Environment*, 30, 1035–1040.
- Silva, W. B., Vicente, M. H., Robledo, J. M., Reartes, D. S., Ferrari, R. C., Bianchetti, R. E., ... Zsögön, A. (2018). SELF-PRUNING Acts Synergistically with DIAGEOTROPICA to guide auxin responses and proper growth form. *Plant Physiology*, 176, 2904–2916.
- Smith, A. M., & Stitt, M. (2007). Coordination of carbon supply and plant growth. *Plant, Cell & Environment*, 30, 1126–1149.

- Stitt, M., Gibon, Y., Lunn, J., & Piques, M. (2007). Multilevel genomics analysis of carbon signaling during diurnal cycles: Balancing supply and utilization by responding to changes in the nonlimiting range. *Functional Plant Biology*, *34*, 526–549.
- Stitt, M., & Zeeman, S. C. (2012). Starch turnover: Pathways, regulation and role in growth. *Current Opinion in Plant Biology*, *15*, 282–292.
- Sulpice, R., Pyl, E.-T., Ishihara, H., Trenkamp, S., Steinfath, M., Witucka-Wall, H., ... Piques, M. C. (2009). Starch as a major integrator in the regulation of plant growth. *Proceedings of the National Academy of Sciences*, *106*, 10348–10353.
- Thimann, K. V. (1977). *Hormone action in the whole life of plants*. Amherst: Univ of Massachusetts Press.
- Vanneste, S., & Friml, J. (2009). Auxin: A trigger for change in plant development. *Cell*, *136*, 1005–1016.
- von Groll, U., Berger, D., & Altmann, T. (2002). The subtilisin-like serine protease SDD1 mediates cell-to-cell signaling during Arabidopsis stomatal development. *The Plant Cell*, *14*, 1527–1539.
- Wang, H., Jones, B., Li, Z., Frasse, P., Delalande, C., Regad, F., ... Bouzayen, M. (2005). The tomato Aux/IAA transcription factor IAA9 is involved in fruit development and leaf morphogenesis. *The Plant Cell Online*, *17*, 2676–2692.
- Wang, H., Schauer, N., Usadel, B., Frasse, P., Zouine, M., Hernould, M., ... Bouzayen, M. (2009). Regulatory features underlying pollination-dependent and-independent tomato fruit set revealed by transcript and primary metabolite profiling. *The Plant Cell*, *21*, 1428–1452.
- Wong, S.-L., Chen, C.-W., Huang, H.-W., & Weng, J.-H. (2012). Using combined measurements of gas exchange and chlorophyll fluorescence to investigate the photosynthetic light responses of plant species adapted to different light regimes. *Photosynthetica*, *50*, 206–214.
- Xu, Z., & Zhou, G. (2008). Responses of leaf stomatal density to water status and its relationship with photosynthesis in a grass. *Journal of Experimental Botany*, *59*, 3317–3325.
- Zanor, M. I., Osorio, S., Nunes-Nesi, A., Carrari, F., Lohse, M., Usadel, B., ... Willmitzer, L. (2009). RNA interference of LIN5 in tomato confirms its role in controlling Brix content, uncovers the influence of sugars on the levels of fruit hormones, and demonstrates the importance of sucrose cleavage for normal fruit development and fertility. *Plant Physiology*, *150*, 1204–1218.
- Zhao, Y. (2010). Auxin biosynthesis and its role in plant development. *Annual Review of Plant Biology*, *61*, 49–64.
- Zheng, H., Li, S., Ren, B., Zhang, J., Ichii, M., Taketa, S., ... Wang, H. (2013). LATERAL ROOTLESS2, a cyclophilin protein, regulates lateral root initiation and auxin signaling pathway in rice. *Molecular Plant*, *6*, 1719–1721.
- Zobel, R. (1973). Some physiological characteristics of the ethylene-requiring tomato mutant diageotropica. *Plant Physiology*, *52*, 385–389.
- Zouine, M., Fu, Y., Chateigner-Boutin, A.-L., Mila, I., Frasse, P., Wang, H., ... Bouzayen, M. (2014). Characterization of the tomato ARF gene family uncovers a multi-levels post-transcriptional regulation including alternative splicing. *PLoS One*, *9*, e84203.

## SUPPORTING INFORMATION

Additional supporting information may be found online in the Supporting Information section at the end of the article.

**How to cite this article:** Batista-Silva W, Medeiros DB, Rodrigues-Salvador A, et al. Modulation of auxin signalling through *DIAGETROPICA* and *ENTIRE* differentially affects tomato plant growth via changes in photosynthetic and mitochondrial metabolism. *Plant Cell Environ*. 2019;42:448–465. <https://doi.org/10.1111/pce.13413>